

6 Kaon mixing

Authors: P. Dimopoulos, X. Feng, G. Herdoíza

The mixing of neutral pseudoscalar mesons plays an important role in the understanding of the physics of quark-flavour mixing and CP violation. In this section, we discuss $K^0 - \bar{K}^0$ oscillations, which probe the physics of indirect CP violation. Extensive reviews on this subject can be found in Refs. [1–6]. The main changes in this section with respect to the FLAG 21 edition [7] are as follows: A discussion on the ϵ_K calculation has been added in Sec. 6.1. An updated discussion regarding new lattice determinations of the $K \rightarrow \pi\pi$ decay amplitudes and related quantities is provided in Sec. 6.2. New FLAG averages for SM and BSM bag parameters are reported in Secs. 6.3 and 6.4, which concern the kaon mixing within the Standard Model (SM) and Beyond the Standard Model (BSM), respectively.

6.1 Indirect CP violation and ϵ_K in the SM

Indirect CP violation arises in $K_L \rightarrow \pi\pi$ transitions through the decay of the CP = +1 component of K_L into two pions (which are also in a CP = +1 state). Its measure is defined as

$$\epsilon_K = \frac{\mathcal{A}[K_L \rightarrow (\pi\pi)_{I=0}]}{\mathcal{A}[K_S \rightarrow (\pi\pi)_{I=0}]} , \quad (82)$$

with the final state having total isospin zero. The parameter ϵ_K may also be expressed in terms of $K^0 - \bar{K}^0$ oscillations. In the Standard Model, ϵ_K is given by the following expression [5, 8–11]

$$\epsilon_K = \exp(i\phi_\epsilon) \sin(\phi_\epsilon) \left[\frac{\text{Im}(M_{12}^{\text{SD}})}{\Delta M_K} + \frac{\text{Im}(M_{12}^{\text{LD}})}{\Delta M_K} + \frac{\text{Im}(A_0)}{\text{Re}(A_0)} \right] , \quad (83)$$

where the various contributions can be related to: (i) short-distance (SD) physics given by $\Delta S = 2$ “box diagrams” involving W^\pm bosons and u, c and t quarks; (ii) long-distance (LD) physics from light hadrons contributing to the imaginary part of the dispersive amplitude M_{12} , $\text{Im}(M_{12}^{\text{LD}})$, used in the two-component description of $K^0 - \bar{K}^0$ mixing; (iii) the imaginary part of the absorptive amplitude Γ_{12} from $K^0 - \bar{K}^0$ mixing which can be related to $\text{Im}(A_0)/\text{Re}(A_0)$, where A_0 is the $K \rightarrow (\pi\pi)_{I=0}$ decay amplitude, as $(\pi\pi)_{I=0}$ states provide the dominant contribution to the absorptive part of the integral in Γ_{12} . The various factors of this decomposition may vary according to phase conventions. In terms of the $\Delta S = 2$ effective Hamiltonian, $\mathcal{H}_{\text{eff}}^{\Delta S=2}$, it is common to represent contribution (i) by

$$\text{Im}(M_{12}^{\text{SD}}) \equiv \frac{1}{2M_K} \text{Im}[\langle \bar{K}^0 | \mathcal{H}_{\text{eff}}^{\Delta S=2} | K^0 \rangle] . \quad (84)$$

The phase of ϵ_K is given by

$$\phi_\epsilon = \arctan \frac{\Delta M_K}{\Delta \Gamma_K / 2} . \quad (85)$$

The quantities ΔM_K and $\Delta \Gamma_K$ are the mass and decay width differences between long- and short-lived neutral kaons. The experimentally known values of the above quantities are [12]:

$$|\epsilon_K| = 2.228(11) \times 10^{-3}, \quad (86)$$

$$\phi_\epsilon = 43.52(5)^\circ, \quad (87)$$

$$\Delta M_K \equiv M_{K_L} - M_{K_S} = 3.484(6) \times 10^{-12} \text{ MeV}, \quad (88)$$

$$\Delta \Gamma_K \equiv \Gamma_{K_S} - \Gamma_{K_L} = 7.3382(33) \times 10^{-12} \text{ MeV}, \quad (89)$$

where the latter three measurements have been obtained by imposing CPT symmetry.

We will start by discussing the short-distance effects (i) since they provide the dominant contribution to ϵ_K . To lowest order in the electroweak theory, the contribution to $K^0 - \bar{K}^0$ oscillations arises from the box diagrams, in which two W bosons and two “up-type” quarks (i.e., up, charm, top) are exchanged between the constituent down and strange quarks of the K mesons. The loop integration of the box diagrams can be performed exactly. In the limit of vanishing external momenta and external quark masses, the result can be identified with an effective four-fermion interaction, expressed in terms of the effective Hamiltonian

$$\mathcal{H}_{\text{eff}}^{\Delta S=2} = \frac{G_F^2 M_W^2}{16\pi^2} \mathcal{F}^0 Q^{\Delta S=2} + \text{h.c.} \quad (90)$$

In this expression, G_F is the Fermi coupling, M_W the W -boson mass, and

$$Q^{\Delta S=2} = [\bar{s}\gamma_\mu(1 - \gamma_5)d][\bar{s}\gamma_\mu(1 - \gamma_5)d] \equiv O_{\text{VV}+\text{AA}} - O_{\text{VA}+\text{AV}}, \quad (91)$$

is a dimension-six, four-fermion operator. The subscripts V and A denote vector ($\bar{s}\gamma_\mu d$) and axial-vector ($\bar{s}\gamma_\mu\gamma_5 d$) bilinears, respectively. The function \mathcal{F}^0 is given by

$$\mathcal{F}^0 = \lambda_c^2 S_0(x_c) + \lambda_t^2 S_0(x_t) + 2\lambda_c\lambda_t S_0(x_c, x_t), \quad (92)$$

where $\lambda_a = V_{as}^* V_{ad}$, and $a = c, t$ denotes a flavour index. The quantities $S_0(x_c)$, $S_0(x_t)$ and $S_0(x_c, x_t)$ with $x_c = m_c^2/M_W^2$, $x_t = m_t^2/M_W^2$ are the Inami-Lim functions [13], which express the basic electroweak loop contributions without QCD corrections. The contribution of the up quark, which is taken to be massless in this approach, has been taken into account by imposing the unitarity constraint $\lambda_u + \lambda_c + \lambda_t = 0$. By substituting $\lambda_c = -\lambda_u - \lambda_t$, one can rewrite \mathcal{F}^0 as [14, 15]

$$\mathcal{F}^0 = \lambda_u^2 S_0(x_c) + \lambda_t^2 [S_0(x_t) + S_0(x_c) - 2S_0(x_c, x_t)] + 2\lambda_u\lambda_t [S_0(x_c) - S_0(x_c, x_t)]. \quad (93)$$

Equations (92) and (93) are denoted as “ c - t unitarity” and “ u - t unitarity”, respectively. Since $\lambda_u^2 S_0(x_c)$ is real, it does not factor into ϵ_K , even when accounting for QCD corrections.

When strong interactions are included, $\Delta S = 2$ transitions can no longer be discussed at the quark level. Instead, the effective Hamiltonian must be considered between mesonic initial and final states. Since the strong coupling is large at typical hadronic scales, the resulting weak matrix element cannot be calculated in perturbation theory. The operator product expansion (OPE) does, however, factorize long- and short-distance effects. For energy scales below the charm threshold, the $K^0 - \bar{K}^0$ transition amplitude of the effective Hamiltonian can be expressed in terms of the c - t unitarity framework as follows

$$\begin{aligned} \langle \bar{K}^0 | \mathcal{H}_{\text{eff}}^{\Delta S=2} | K^0 \rangle &= \frac{G_F^2 M_W^2}{16\pi^2} \left[\lambda_c^2 S_0(x_c) \eta_1 + \lambda_t^2 S_0(x_t) \eta_2 + 2\lambda_c\lambda_t S_0(x_c, x_t) \eta_3 \right] \\ &\times \left(\frac{\bar{g}(\mu)^2}{4\pi} \right)^{-\gamma_0/(2\beta_0)} \exp \left\{ \int_0^{\bar{g}(\mu)} dg \left(\frac{\gamma(g)}{\beta(g)} + \frac{\gamma_0}{\beta_0 g} \right) \right\} \langle \bar{K}^0 | Q_R^{\Delta S=2}(\mu) | K^0 \rangle + \text{h.c.}, \quad (94) \end{aligned}$$

where $\bar{g}(\mu)$ and $Q_R^{\Delta S=2}(\mu)$ are the renormalized gauge coupling and the four-fermion operator in some renormalization scheme. The factors η_1, η_2 and η_3 depend on the renormalized coupling \bar{g} , evaluated at the various flavour thresholds m_t, m_b, m_c and M_W , as required by the OPE and Renormalization-Group (RG) running procedure that separate high- and low-energy contributions. Explicit expressions can be found in Ref. [4] and references therein, except that η_1 and η_3 have been calculated to NNLO in Refs. [16] and [17], respectively. We follow the same conventions for the RG equations as in Ref. [4]. Thus the Callan-Symanzik function and the anomalous dimension $\gamma(\bar{g})$ of $Q^{\Delta S=2}$ are defined by

$$\frac{d\bar{g}}{d\ln\mu} = \beta(\bar{g}), \quad \frac{dQ_R^{\Delta S=2}}{d\ln\mu} = -\gamma(\bar{g}) Q_R^{\Delta S=2}, \quad (95)$$

with perturbative expansions

$$\begin{aligned} \beta(g) &= -\beta_0 \frac{g^3}{(4\pi)^2} - \beta_1 \frac{g^5}{(4\pi)^4} - \dots, \\ \gamma(g) &= \gamma_0 \frac{g^2}{(4\pi)^2} + \gamma_1 \frac{g^4}{(4\pi)^4} + \dots. \end{aligned} \quad (96)$$

We stress that β_0, β_1 and γ_0 are universal, i.e., scheme independent. As for $K^0 - \bar{K}^0$ mixing, this is usually considered in the naive dimensional regularization (NDR) scheme of $\overline{\text{MS}}$, and below we specify the perturbative coefficient γ_1 in that scheme:

$$\begin{aligned} \beta_0 &= \left\{ \frac{11}{3}N - \frac{2}{3}N_f \right\}, \quad \beta_1 = \left\{ \frac{34}{3}N^2 - N_f \left(\frac{13}{3}N - \frac{1}{N} \right) \right\}, \\ \gamma_0 &= \frac{6(N-1)}{N}, \quad \gamma_1 = \frac{N-1}{2N} \left\{ -21 + \frac{57}{N} - \frac{19}{3}N + \frac{4}{3}N_f \right\}. \end{aligned} \quad (97)$$

Note that for QCD the above expressions must be evaluated for $N = 3$ colours, while N_f denotes the number of active quark flavours. As already stated, Eq. (94) is valid at scales below the charm threshold, after all heavier flavours have been integrated out, i.e., $N_f = 3$.

In Eq. (94), the terms proportional to η_1, η_2 and η_3 , multiplied by the contributions containing $\bar{g}(\mu)^2$, correspond to the Wilson coefficient of the OPE, computed in perturbation theory. Its dependence on the renormalization scheme and scale μ is canceled by that of the weak matrix element $\langle \bar{K}^0 | Q_R^{\Delta S=2}(\mu) | K^0 \rangle$. The latter corresponds to the long-distance effects of the effective Hamiltonian and must be computed nonperturbatively. For historical, as well as technical reasons, it is convenient to express it in terms of the B -parameter B_K , defined as

$$B_K(\mu) = \frac{\langle \bar{K}^0 | Q_R^{\Delta S=2}(\mu) | K^0 \rangle}{\frac{8}{3} f_K^2 M_K^2}. \quad (98)$$

The four-quark operator $Q^{\Delta S=2}(\mu)$ is renormalized at scale μ in some regularization scheme, for instance, NDR- $\overline{\text{MS}}$. Assuming that $B_K(\mu)$ and the anomalous dimension $\gamma(g)$ are both known in that scheme, the renormalization group independent (RGI) B -parameter \hat{B}_K is related to $B_K(\mu)$ by the exact formula

$$\hat{B}_K = \left(\frac{\bar{g}(\mu)^2}{4\pi} \right)^{-\gamma_0/(2\beta_0)} \exp \left\{ \int_0^{\bar{g}(\mu)} dg \left(\frac{\gamma(g)}{\beta(g)} + \frac{\gamma_0}{\beta_0 g} \right) \right\} B_K(\mu). \quad (99)$$

At NLO in perturbation theory, the above reduces to

$$\hat{B}_K = \left(\frac{\bar{g}(\mu)^2}{4\pi} \right)^{-\gamma_0/(2\beta_0)} \left\{ 1 + \frac{\bar{g}(\mu)^2}{(4\pi)^2} \left[\frac{\beta_1\gamma_0 - \beta_0\gamma_1}{2\beta_0^2} \right] \right\} B_K(\mu) . \quad (100)$$

To this order, this is the scale-independent product of all μ -dependent quantities in Eq. (94).

Lattice-QCD calculations provide results for $B_K(\mu)$. However, these results are usually obtained in intermediate schemes other than the continuum $\overline{\text{MS}}$ scheme used to calculate the Wilson coefficients appearing in Eq. (94). Examples of intermediate schemes are the RI/MOM scheme [18] (also dubbed the “Rome-Southampton method”) and the Schrödinger functional (SF) scheme [19]. These schemes permit the nonperturbative renormalization of the four-fermion operator to be conducted, using an auxiliary lattice simulation. This allows $B_K(\mu)$ to be calculated with percent-level accuracy, as described below.

In order to make contact with phenomenology, however, and in particular to use the results presented above, one must convert from the intermediate scheme to the $\overline{\text{MS}}$ scheme or to the RGI quantity \hat{B}_K . This conversion relies on 1- or 2-loop perturbative matching calculations, the truncation errors in which are, for many calculations, the dominant source of error in \hat{B}_K (see, for instance, Refs. [20–25]). While this scheme-conversion error is not, strictly speaking, an error of the lattice calculation itself, it must be included in results for the quantities of phenomenological interest, namely, $B_K(\overline{\text{MS}}, 2 \text{ GeV})$ and \hat{B}_K . Incidentally, we remark that this truncation error is estimated in different ways and that its relative contribution to the total error can considerably differ among the various lattice calculations. We note that this error can be minimized by matching between the intermediate scheme and $\overline{\text{MS}}$ at as large a scale μ as possible (so that the coupling which determines the rate of convergence is minimized). The latest available calculations have pushed the matching μ up to the range 3–3.5 GeV. This is possible because of the use of nonperturbative RG running determined on the lattice [21, 23, 26]. The Schrödinger functional offers the possibility to run nonperturbatively to scales $\mu \sim M_W$ where the truncation error can be safely neglected. However, so far this has been applied only for two flavours for B_K in Ref. [27] and for the case of the BSM bag parameters in Ref. [28], and in Ref. [29] for three flavours. (See more details in Sec. 6.4.)

Perturbative truncation errors in Eq. (94) also affect the Wilson coefficients η_1 , η_2 and η_3 . It turns out that the largest uncertainty arises from the charm quark contribution $\eta_1 = 1.87(76)$ [16]. Although it is now calculated at NNLO, the series shows poor convergence. The net effect from the uncertainty on η_1 on the amplitude in Eq. (94) is larger than that of present lattice calculations of B_K . Exploiting an idea presented in Ref. [14], it has been shown in Ref. [15] that, by using the u - t instead of the usual c - t unitarity in the ϵ_K computation, the perturbative uncertainties associated with residual short-distance quark contributions can be reduced. We will elaborate upon this point later.

Returning to Eq. (83), we note that an analytical estimate of the leading contribution from $\text{Im}(M_{12}^{\text{LD}})$ based on χ PT, shows that it is approximately proportional to $\xi_0 \equiv \text{Im}(A_0)/\text{Re}(A_0)$ so that Eq. (83) can be written as follows [10, 11]:

$$\epsilon_K = \exp(i\phi_\epsilon) \sin(\phi_\epsilon) \left[\frac{\text{Im}(M_{12}^{\text{SD}})}{\Delta M_K} + \rho \xi_0 \right], \quad (101)$$

where the deviation of ρ from one parameterizes the long-distance effects in $\text{Im}(M_{12})$.

The general formula presented in Eq. (101) for the parameter ϵ_K provides one of the most valuable inputs for tests of CKM unitarity. Moreover, it holds significant potential as a probe for New Physics, provided that its precision can be enhanced. In the following, we will provide a general overview of the current status of the computation of $|\epsilon_K|$.

With a very good approximation the formula for $|\epsilon_K|$ can be written in the so-called Wolfenstein parametrization [30]. The determination of $|\epsilon_K|$ requires the knowledge of more than a dozen input quantities, which can be categorized into four groups. The first group includes six quantities (G_F , ϕ_ϵ , M_{K^0} , ΔM_K , M_W and m_t) whose values are known from experiment with high precision. The second group consists of several observables computed in lattice QCD, including the kaon decay constant f_K , the charm-quark mass $m_c(m_c)$, the neutral kaon mixing bag parameter B_K , and the ratio $\xi_0 = \text{Im}(A_0)/\text{Re}(A_0)$.¹ Moreover, the values of the CKM matrix elements $|V_{ud}|$, $|V_{us}|$ and $|V_{cb}|$ are required—see for instance Ref. [32]—which are based on lattice-QCD computations. It is worth recalling that the present FLAG report provides average values for these quantities, see Secs. 5 and 8. The third group involves the short-distance interaction factors calculated in perturbation theory. In the c - t unitarity formula, these factors are η_1 , η_2 , and η_3 , as mentioned earlier in this section and shown in Eq. (94). In the u - t unitarity case, there appear only two relevant factors (see Refs. [15, 33]). Finally, the fourth group of inputs consists of the pair of CKM triangle variables $(\bar{\rho}, \bar{\eta})$ whose values are estimated from the unitarity triangle analysis. In particular, the Angle-only Fit (AoF) analysis used in Refs. [34–36] (see also Ref. [37]) prevents any correlation of $(\bar{\rho}, \bar{\eta})$ with the rest of the inputs used in the formula for $|\epsilon_K|$.

Among the various inputs the value of $|V_{cb}|$ has a dominant impact on the uncertainty of $|\epsilon_K|$ because $|V_{cb}|$ appears to the fourth power in the expression of $|\epsilon_K|$. Among the various inputs, $|V_{cb}|$ introduces the dominant contribution on the uncertainty of $|\epsilon_K|$. This effect can be attributed to the presence of terms with $|V_{cb}|$ to the fourth and second power in the expression of $|\epsilon_K|$.

As discussed in Sec. 8 of this report, to which we refer for a comprehensive review, a longstanding discrepancy persists between the exclusive and inclusive determinations of $|V_{cb}|$. Exclusive determinations, which are primarily based on the differential decay rates of processes such as $B \rightarrow D^* \ell \nu$ and $B \rightarrow D \ell \nu$, rely on nonperturbative inputs from lattice QCD. In contrast, inclusive determinations employ the total semileptonic decay rate $B \rightarrow X_c \ell \nu$ and are analysed within the framework of heavy quark effective theory and the operator product expansion. The application of these two types of theoretical approaches, in conjunction with distinct experimental inputs, yields the current sizeable tension between the exclusive and inclusive determinations of $|V_{cb}|$.

Another significant source of uncertainty, when the c - t unitarity formula for $|\epsilon_K|$ is employed, is related to the factor η_1 that is computed to NNLO in perturbation theory. For more information on the estimation of the systematic error due to perturbative truncation, see Refs. [16, 35, 38]. This source of uncertainty can be mitigated by adopting the u - t unitarity formula for $|\epsilon_K|$. In this case, it is found that the two relevant QCD perturbative factors are not subject to significant systematic uncertainties. Furthermore, this approach reduces the correlations between the individual perturbative contributions [15].

We close this discussion by mentioning that the use of the u - t unitarity formula leads to a

¹Furthermore, the long-distance effects owing to light hadrons can be estimated on the lattice as noted below in Sec. 6.2, c.f. Ref. [31]. However, the current accuracy of this calculation is not yet high enough to constrain the determination of $|\epsilon_K|$.

total statistical error of about 8% in $|\epsilon_K|$. In this case, when analyzing the error budget, we see that nearly half of the total error comes from the propagation of the uncertainty from $|V_{cb}|$. Furthermore, the propagated error owing to the $\bar{\eta}$ error is the second most significant source of uncertainty in $|\epsilon_K|$. It is noteworthy that the propagated error from B_K is much smaller, accounting for only a few percent in the final error budget. It should also be noted that the relative uncertainties contributing to the error budget are rather sensitive to improvements in the precision of $|V_{cb}|$. The tension between the exclusive and inclusive determinations of $|V_{cb}|$ induces a corresponding difference in the predicted values of $|\epsilon_K|$ derived from these inputs. Recent detailed analyses of $|\epsilon_K|$, including the impact of different $|V_{cb}|$ determinations and the use of the c - t and u - t unitarity relations, can be found in Refs. [32, 39, 40]. It is also worth noting that ongoing advancements in lattice-QCD techniques may contribute in the future to reducing uncertainties in the inclusive determination of $|V_{cb}|$ [41–45]. The resolution of the longstanding discrepancy between the exclusive and inclusive determinations of $|V_{cb}|$ is highly desirable, as it would significantly enhance the precision of $|\epsilon_K|$ and its potential for probing New Physics scenarios.²

In order to facilitate the subsequent discussions about the status of the lattice studies of $K \rightarrow \pi\pi$ and of the current estimates of $\xi_0 \equiv \text{Im}(A_0)/\text{Re}(A_0)$, we provide a brief account of the parameter ϵ' that describes direct CP-violation in the kaon sector. The definition of ϵ' is given by:

$$\epsilon' \equiv \frac{1}{\sqrt{2}} \frac{\mathcal{A}[K_S \rightarrow (\pi\pi)_{I=2}]}{\mathcal{A}[K_S \rightarrow (\pi\pi)_{I=0}]} \left(\frac{\mathcal{A}[K_L \rightarrow (\pi\pi)_{I=2}]}{\mathcal{A}[K_S \rightarrow (\pi\pi)_{I=2}]} - \frac{\mathcal{A}[K_L \rightarrow (\pi\pi)_{I=0}]}{\mathcal{A}[K_S \rightarrow (\pi\pi)_{I=0}]} \right). \quad (102)$$

By selecting appropriate phase conventions for the mixing parameters between K^0 and \bar{K}^0 CP-eigenstates (see, e.g., Ref. [2] for further details), the expression of ϵ' can be expressed in terms of the real and imaginary parts of the isospin amplitudes as follows:

$$\epsilon' = \frac{i\omega e^{i(\delta_2 - \delta_0)}}{\sqrt{2}} \left[\xi_2 - \xi_0 \right], \quad (103)$$

where $\omega \equiv \text{Re}(A_2)/\text{Re}(A_0)$, $\xi_2 \equiv \text{Im}(A_2)/\text{Re}(A_2)$, A_2 denotes the $\Delta I = 3/2$ $K \rightarrow \pi\pi$ decay amplitude, and δ_I denotes the strong scattering phase shifts in the corresponding, $I = 0, 2$, $K \rightarrow (\pi\pi)_I$ decays. Given that the phase $\phi'_\epsilon = \delta_2 - \delta_0 + \pi/2 \approx 42.3(1.5)^\circ$ [12] is nearly equal to ϕ_ϵ in Eq. (87), the ratio of parameters characterizing the direct and indirect CP-violation in the kaon sector can be approximated in the following way,

$$\epsilon'/\epsilon \approx \text{Re}(\epsilon'/\epsilon) = \frac{\omega}{\sqrt{2}|\epsilon_K|} \left[\xi_2 - \xi_0 \right], \quad (104)$$

where on the left hand side we have set $\epsilon \equiv \epsilon_K$. The experimentally measured value reads [12],

$$\text{Re}(\epsilon'/\epsilon) = 16.6(2.3) \times 10^{-4}. \quad (105)$$

We remark that isospin breaking and electromagnetic effects (see Refs. [48, 49], and the discussion in Ref. [3]) introduce additional correction terms into Eq. (104).

²Note that a more precise determination of $|\epsilon_K|$ will require taking into account the effect of short-distance power corrections from dim-8 operators to the $\Delta S = 2$ effective Hamiltonian. It is estimated that their effect leads to an increase of the central value by 1%, see Refs. [46, 47].

6.2 Lattice-QCD studies of the $K \rightarrow (\pi\pi)_I$ decay amplitudes, ξ_0 , ξ_2 and ϵ'/ϵ

As a preamble to this section, it should be noted that the study of $K \rightarrow \pi\pi$ decay amplitudes requires the development of computational strategies that are at the forefront of lattice QCD techniques. These studies represent a significant advance in the study of kaon physics. However, at present, they have not yet reached the same level of maturity of most of the quantities analyzed in the FLAG report, where, for instance, independent results by various lattice collaborations are being compared and averaged. We will, therefore, review the current status of $K \rightarrow \pi\pi$ lattice computations, but we will provide a FLAG average only for the case of the decay amplitude A_2 .

We start by reviewing the determination of the parameter $\xi_0 = \text{Im}(A_0)/\text{Re}(A_0)$. An estimate of ξ_0 has been obtained from a direct evaluation of the ratio of amplitudes $\text{Im}(A_0)/\text{Re}(A_0)$, where $\text{Im}(A_0)$ is determined from a lattice-QCD computation by RBC/UKQCD 20 [50] employing $N_f = 2 + 1$ Möbius domain-wall fermions at a single value of the lattice spacing, while $\text{Re}(A_0) \simeq |A_0|$ and the value $|A_0| = 3.320(2) \times 10^{-7}$ GeV are used based on the relevant experimental input [51] from the decay to two pions. This leads to a result for ξ_0 with a rather large relative error,

$$\xi_0 = -2.1(5) \times 10^{-4}. \quad (106)$$

Following a similar procedure, an estimate of ξ_0 was obtained through the use of a previous lattice QCD determination of $\text{Im}(A_0)$ by RBC/UKQCD 15G [52]. We refer to Tab. 22 for further details about these computations of $\text{Im}(A_0)$. The comparison of the estimates of ξ_0 based on lattice QCD input are collected in Tab. 24.

To determine the value of ξ_0 , the expression in Eq. (104) together with the experimental values of $\text{Re}(\epsilon'/\epsilon)$, $|\epsilon_K|$ and ω can also be used. This approach has been pursued with the help of a lattice-QCD calculation of the ratio of amplitudes $\text{Im}(A_2)/\text{Re}(A_2)$ by RBC/UKQCD 15F [53] where the continuum-limit result is based on computations at two values of the lattice spacing employing $N_f = 2 + 1$ Möbius domain-wall fermions. Further details about the lattice computations of A_2 are collected in Tab. 23. In this case, we obtain $\xi_0 = -1.6(2) \times 10^{-4}$. The use of the updated value of $\text{Im}(A_2) = -8.34(1.03) \times 10^{-13}$ GeV from Ref. [50], in combination with the experimental value of $\text{Re}(A_2) = 1.479(4) \times 10^{-8}$ GeV, introduces a small change with respect to the above result.³ The value for ξ_0 reads⁴

$$\xi_0 = -1.7(2) \times 10^{-4}. \quad (107)$$

A phenomenological estimate can also be obtained from the relationship of ξ_0 to $\text{Re}(\epsilon'/\epsilon)$, using the experimental value of the latter and further assumptions concerning the estimate of hadronic contributions. The corresponding value of ξ_0 reads [10, 11]

$$\xi_0 = -6.0(1.5) \times 10^{-2} \times \sqrt{2} |\epsilon_K| = -1.9(5) \times 10^{-4}. \quad (108)$$

³The update in $\text{Im}(A_2)$ is due to a change in the value of the imaginary part of the ratio of CKM matrix elements, $\tau = -V_{ts}^* V_{td}/V_{us}^* V_{ud}$, as given in Ref. [54]. The lattice-QCD input is therefore the one reported in Ref. [53].

⁴The current estimates for the corrections owing to isospin breaking and electromagnetic effects [49] imply a relative change on the theoretical value for ϵ'/ϵ by about -20% with respect to the determination based on Eq. (104). The size of these isospin breaking and electromagnetic corrections is related to the enhancement of the decay amplitudes between the $I = 0$ and the $I = 2$ channels. As a consequence, one obtains a similar reduction on ξ_0 , leading to a value that is close to the result of Eq. (106).

We note that the use of the experimental value for $\text{Re}(\epsilon'/\epsilon)$ is based on the assumption that it is free from New Physics contributions. The value of ξ_0 can then be combined with a χ PT-based estimate for the long-range contribution, $\rho = 0.6(3)$ [11]. Overall, the combination $\rho\xi_0$ appearing in Eq. (101) leads to a suppression of the SM prediction of $|\epsilon_K|$ by about 3(2)% relative to the experimental measurement of $|\epsilon_K|$ given in Eq. (86), regardless of whether the phenomenological estimate of ξ_0 [see Eq. (108)] or the most precise lattice result [see Eq. (106)] are used. The uncertainty in the suppression factor is dominated by the error on ρ . Although this is a small correction, we note that its contribution to the error of ϵ_K is larger than that arising from the value of B_K reported below.

The evolution of lattice-QCD methodologies has enabled recent ongoing efforts to calculate the long-distance contributions to ϵ_K [31, 55] and the $K_L - K_S$ mass difference [14, 56–59]. However, the results are not yet precise enough to improve the accuracy in the determination of the parameter ρ .

The lattice-QCD study of $K \rightarrow \pi\pi$ decays provides crucial input to the SM prediction of ϵ_K . During the last decade, the RBC/UKQCD collaboration has undertaken a series of lattice-QCD calculations of $K \rightarrow \pi\pi$ decay amplitudes [50, 52, 53, 60]. In 2015, the first calculation of the $K \rightarrow (\pi\pi)_{I=0}$ decay amplitude A_0 was performed using physical kinematics on a $32^3 \times 64$ lattice with an inverse lattice spacing of $a^{-1} = 1.3784(68)$ GeV [52, 61]. The main features of the RBC/UKQCD 15G calculation included, fixing the $I = 0$ $\pi\pi$ energy very close to the kaon mass by imposing G-parity boundary conditions, a continuum-like operator mixing pattern through the use of a domain-wall fermion action with accurate chiral symmetry, and the construction of the complete set of correlation functions by computing seventy-five distinct diagrams. Results for the real and the imaginary parts of the decay amplitude A_0 from the RBC/UKQCD 15G computation are collected in Tab. 22, where the first error is statistical and the second is systematic.

The calculation in RBC/UKQCD 20 [50] using the same lattice setup has improved upon RBC/UKQCD 15G [52] in three important aspects: (i) an increase in statistics by a factor of 3.4; (ii) the inclusion of a scalar two-quark operator and the addition of another pion-pion operator to isolate the ground state, and (iii) the use of step scaling techniques to raise the renormalization scale from 1.53 GeV to 4.01 GeV. The updated determinations of the real and the imaginary parts of A_0 in Ref. [50] are shown in Tab. 22.

In addition to utilizing G-parity boundary conditions to address the challenges associated with extracting excited states for achieving the correct kinematics of $K \rightarrow \pi\pi$, the latest publications, RBC/UKQCD 23A [60] and RBC/UKQCD 23B [62], also investigate alternative approaches for overcoming this issue, namely employing variational methods and periodic boundary conditions. Two-pion scattering calculations are carried out for the isospin channels $I = 0$ and $I = 2$ on two gauge-field ensembles with physical pion masses and inverse lattice spacings of 1.023 and 1.378 GeV [62] employing domain-wall fermions. The results for scattering phase shifts in both $I = 0$ and $I = 2$ channels exhibit consistency with the Roy equation and chiral perturbation theory, although the statistical error for $I = 0$ remains relatively large. The computation of $K \rightarrow \pi\pi$ decay amplitudes and ϵ' is performed on a single ensemble with a physical pion mass and an inverse lattice spacing of 1.023 GeV [60]. The value obtained for $\text{Re}(\epsilon'/\epsilon)$ is consistent with that of the previous 2020 calculation, albeit with 1.7 times larger uncertainty. Results from RBC/UKQCD 23A for the real and imaginary parts of A_0 and A_2 are reported in Tabs. 22 and 23, respectively.

As previously discussed, the determination of $\text{Im}(A_0)$ from Ref. [50] has been used to obtain the value of the parameter ξ_0 in Eq. (106). A first-principles computation of $\text{Re}(A_0)$

Collaboration	Ref.	N_f	publication status	continuum extrapolation	chiral extrapolation	finite volume	renormalization	running/matching	$\text{Re}(A_0)$ [10^{-7} GeV]	$\text{Im}(A_0)$ [10^{-11} GeV]
RBC/UKQCD 23A	[60]	2+1	A	■	○	★	★	<i>a</i>	2.84(0.57)(0.87)	−8.7(1.2)(2.6)
RBC/UKQCD 20	[50]	2+1	A	■	○	○	★	<i>a</i>	2.99(0.32)(0.59)	−6.98(0.62)(1.44)
RBC/UKQCD 15G	[52]	2+1	A	■	○	○	★	<i>b</i>	4.66(1.00)(1.26)	−1.90(1.23)(1.08)

a Nonperturbative renormalization with the RI/SMOM scheme at a scale of 1.53 GeV and running to 4.0 GeV employing a nonperturbatively determined step-scaling function. Conversion to $\overline{\text{MS}}$ at 1-loop order.

b Nonperturbative renormalization with the RI/SMOM scheme at a scale of 1.53 GeV. Conversion to $\overline{\text{MS}}$ at 1-loop order at the same scale.

Table 22: Results for the real and imaginary parts of the $K \rightarrow \pi\pi$ decay amplitude A_0 from lattice-QCD computations with $N_f = 2 + 1$ dynamical flavours. Information about the renormalization, running and matching to the $\overline{\text{MS}}$ scheme is indicated in the column “running/matching”, with details given at the bottom of the table. We refer to the text for further details about the main differences between the lattice computations in Refs. [50] and [52].

is essential to address the so-called $\Delta I = 1/2$ puzzle associated to the enhancement of $\Delta I = 1/2$ over $\Delta I = 3/2$ transitions owing, crucially, to long distance effects. Indeed, short-distance enhancements in the Wilson coefficients are not large enough to explain the $\Delta I = 1/2$ rule [63, 64]. Lattice-QCD calculations do provide a method to study such a long-distance enhancement. The combination of the most precise result for A_0 in Tab. 22, Ref. [50], with the earlier lattice calculation of A_2 in Ref. [53] leads to the ratio, $\text{Re}(A_0)/\text{Re}(A_2) = 19.9(5.0)$, which agrees with the value $\text{Re}(A_0)/\text{Re}(A_2) = 22.45(6)$ that we obtain based solely on PDG 24 [12] experimental input. In Ref. [50], the lattice determination of relative size of direct CP violation was updated as follows,

$$\text{Re}(\epsilon'/\epsilon) = 21.7(2.6)(6.2)(5.0) \times 10^{-4}, \quad (109)$$

where the first two errors are statistical and systematic, respectively. The third error arises from having omitted the strong and electromagnetic isospin breaking effects. The value of $\text{Re}(\epsilon'/\epsilon)$ in Eq. (109) uses the experimental values of $\text{Re}(A_0)$ and $\text{Re}(A_2)$. The lattice determination of $\text{Re}(\epsilon'/\epsilon)$ is in good agreement with the experimental result in Eq. (105). However, while the result in Eq. (109) represents a significant step forward, it is important to keep in mind that the calculation of A_0 is currently based on a single value of the lattice spacing. It is expected that future work with additional values of the lattice spacing will contribute to improve the precision. For a description of the computation of the $\pi\pi$ scattering phase shifts entering in the determination of $\text{Re}(\epsilon'/\epsilon)$ in Eq. (109), we refer to Ref. [65].

The complex amplitude A_2 has been determined by RBC/UKQCD 15F [53] employing $N_f = 2 + 1$ Möbius domain-wall fermions at two values of the lattice spacing, namely $a =$

Collaboration	Ref.	N_f		publication status	continuum extrapolation	chiral extrapolation	finite volume	renormalization	running/matching	$\text{Re}(A_2)$ [10^{-8} GeV]	$\text{Im}(A_2)$ [10^{-13} GeV]
RBC/UKQCD 23A	[60]	2+1	A	■	○	★	★	<i>a</i>		1.74(0.15)(0.48)	-5.91(0.13)(1.75)
RBC/UKQCD 15F	[53]	2+1	A	○	○	★	★	<i>b</i>		1.50(0.04)(0.14)	-8.34(1.03) [◇]

a Nonperturbative renormalization with the RI/SMOM scheme at a scale of 1.53 GeV and running to 4.0 GeV employing a nonperturbatively determined step-scaling function. Conversion to $\overline{\text{MS}}$ at 1-loop order.

b Nonperturbative renormalization with the RI/SMOM scheme at a scale of 3 GeV. Conversion to $\overline{\text{MS}}$ at 1-loop order.

◇ This value of $\text{Im}(A_2)$ is an update reported in Ref. [50] which is based on the lattice QCD computation in Ref. [53] but where a change in the value of the imaginary part of the ratio of CKM matrix elements $\tau = -V_{ts}^* V_{td}/V_{us}^* V_{ud}$ reported in Ref. [54] has been applied.

Table 23: Results for the real and the imaginary parts of the $K \rightarrow \pi\pi$ decay amplitude A_2 from lattice-QCD computations with $N_f = 2 + 1$ dynamical flavours. Information about the renormalization and matching to the $\overline{\text{MS}}$ scheme is indicated in the column “running/matching”, with details given at the bottom of the table.

0.114 fm and 0.083 fm, and performing simulations at the physical pion mass with $M_\pi L \approx 3.8$.

A compilation of lattice results for the real and imaginary parts of the $K \rightarrow \pi\pi$ decay amplitudes, A_0 and A_2 , with $N_f = 2 + 1$ flavours of dynamical quarks is shown in Tabs. 22 and 23. In Appendix C.3.3, we collect the corresponding information about the lattice QCD simulations, including the values of some of the most relevant parameters.

The determination of the real and imaginary parts of A_2 by RBC/UKQCD 15F shown in Tab. 23 is free of red tags. We therefore quote the following FLAG averages:

$$\begin{aligned}
 N_f = 2 + 1 : \quad & \text{Re}(A_2) = 1.50(0.04)(0.14) \times 10^{-8} \text{ GeV}, \\
 & \text{Im}(A_2) = -8.34(1.03) \times 10^{-13} \text{ GeV},
 \end{aligned}
 \quad \text{Ref. [53]}. \quad (110)$$

Results for the parameter ξ_0 are presented in Tab. 24. Except for the most recent calculation RBC/UKQCD 23A, which is based on the direct lattice calculation of the relevant quantities, we note that, for the other reported values of ξ_0 , the total uncertainty depends on the specific way in which lattice and experimental inputs are selected.

Besides the RBC/UKQCD collaboration programme [50, 52, 53, 60, 62] using domain-wall fermions, an approach based on improved Wilson fermions [66, 67] has presented a determination of the $K \rightarrow \pi\pi$ decay amplitudes, A_0 and A_2 , at unphysical quark masses. See Refs. [68–70] for an analysis of the scaling with the number of colours of $K \rightarrow \pi\pi$ decay amplitudes using lattice-QCD computations

Proposals aiming at the inclusion of electromagnetism in lattice-QCD calculations of $K \rightarrow \pi\pi$ decays are being explored [71–73] in order to reduce the uncertainties associated with isospin breaking effects.

Collaboration	Ref.	N_f	ξ_0
RBC/UKQCD 23A [◦]	[60]	2+1	$-2.63(37)(68) \cdot 10^{-4}$
RBC/UKQCD 20 [†]	[50]	2+1	$-2.1(5) \cdot 10^{-4}$
RBC/UKQCD 15G [◊]	[52]	2+1	$-0.6(5) \cdot 10^{-4}$
RBC/UKQCD 15F [*]	[53]	2+1	$-1.7(2) \cdot 10^{-4}$

[◦] Estimate for ξ_0 has been provided by RBC/UKQCD (private communication with Masaaki Tomii.)

[†] Estimate for ξ_0 obtained from a direct evaluation of the ratio of amplitudes $\text{Im}(A_0)/\text{Re}(A_0)$ where $\text{Im}(A_0)$ is determined from the lattice-QCD computation of Ref. [50] while for $\text{Re}(A_0) \simeq |A_0|$ is taken from the experimental value for $|A_0|$.

[◊] Estimate for ξ_0 obtained from a direct evaluation of the ratio of amplitudes $\text{Im}(A_0)/\text{Re}(A_0)$ where $\text{Im}(A_0)$ is determined from the lattice-QCD computation of Ref. [52] while for $\text{Re}(A_0) \simeq |A_0|$ is taken from the experimental value for $|A_0|$.

^{*} Estimate for ξ_0 based on the use of Eq. (104). The new value of $\text{Im}(A_2)$ reported in Ref. [50]—based on the lattice-QCD computation of Ref. [53] following an update of a nonlattice input—is used in combination with the experimental values for $\text{Re}(A_2)$, $\text{Re}(\epsilon'/\epsilon)$, $|\epsilon_K|$ and ω .

Table 24: Results for the parameter $\xi_0 = \text{Im}(A_0)/\text{Re}(A_0)$ obtained through the combination of lattice-QCD determinations of $K \rightarrow \pi\pi$ decay amplitudes with $N_f = 2 + 1$ dynamical flavours and experimental inputs.

6.3 Lattice computation of B_K

Lattice calculations of B_K are affected by the same type of systematic effects discussed in the various sections of this review. However, the issue of renormalization merits special attention. The reason is that the multiplicative renormalizability of the relevant operator $Q^{\Delta S=2}$ is lost once the regularized QCD action ceases to be invariant under chiral transformations. As a result, the renormalization pattern of B_K depends on the specific choice of the fermionic discretization.

In the case of Wilson fermions, $Q^{\Delta S=2}$ mixes with four additional dimension-six operators, which belong to different representations of the chiral group, with mixing coefficients that are finite functions of the gauge coupling. This complicated renormalization pattern was identified as the main source of systematic error in earlier, mostly quenched calculations of B_K with Wilson quarks. It can be bypassed via the implementation of specifically designed methods, which are either based on Ward identities [74] or on a modification of the Wilson quark action, known as twisted-mass QCD [75–77].

An advantage of staggered fermions is the presence of a remnant $U(1)$ chiral symmetry. However, at nonvanishing lattice spacing, the symmetry among the extra unphysical degrees of freedom (tastes) is broken. As a result, mixing with other dimension-six operators cannot be avoided in the staggered formulation, which complicates the determination of the B -parameter. In general, taste conserving mixings are implemented directly in the lattice computation of the matrix element. The effects of the broken taste symmetry are usually treated through an effective field theory, staggered Chiral Perturbation Theory ($S\chi\text{PT}$) [78, 79], parameterizing the quark-mass and lattice-spacing dependences.

Fermionic lattice actions based on the Ginsparg-Wilson relation [80] are invariant under the chiral group, and hence four-quark operators such as $Q^{\Delta S=2}$ renormalize multiplicatively. However, depending on the particular formulation of Ginsparg-Wilson fermions, residual chiral symmetry breaking effects may be present in actual calculations. For instance, in the case of domain-wall fermions, the finiteness of the extra 5th dimension implies that the decoupling of modes with different chirality is not exact, which produces a residual nonzero quark mass m_{res} in the chiral limit. The mixing with dimension-six operators of different chirality is expected to be an $\mathcal{O}(m_{\text{res}}^2)$ suppressed effect [81, 82] that should be investigated on a case-by-case basis.

Before describing the results for B_K , we would like to reiterate a discussion presented in previous FLAG reports about an issue related to the computation of the kaon bag parameters through lattice-QCD simulations with $N_f = 2 + 1 + 1$ dynamical quarks. In practice, this only concerns the calculations of the kaon B -parameters including dynamical charm-quark effects in Ref. [83], that were examined in the FLAG 16 report. As described in Sec. 6.1, the effective Hamiltonian in Eq. (90) depends solely on the operator $Q^{\Delta S=2}$ in Eq. (91) —which appears in the definition of B_K in Eq. (98)— at energy scales below the charm threshold where charm-quark contributions are absent. As a result, a computation of B_K based on $N_f = 2 + 1 + 1$ dynamical simulations will include an extra sea-quark contribution from charm-quark loop effects for which there is at present no direct evaluation in the literature.

When the matrix element of $Q^{\Delta S=2}$ is evaluated in a theory that contains a dynamical charm quark, the resulting estimate for B_K must then be matched to the three-flavour theory that underlies the effective four-quark interaction.⁵ In general, the matching of $2 + 1$ -flavour QCD with the theory containing $2 + 1 + 1$ flavours of sea quarks is performed around the charm threshold. It is usually accomplished by requiring that the coupling and quark masses are equal in the two theories at a renormalization scale μ around m_c . In addition, B_K should be renormalized and run, in the four-flavour theory, to the value of μ at which the two theories are matched, as described in Sec. 6.1. The corrections associated with this matching are of order $(E/m_c)^2$, where E is a typical energy in the process under study, since the subleading operators have dimension eight [84].

When the kaon-mixing amplitude is considered, the matching also involves the relation between the relevant box diagrams and the effective four-quark operator. In this case, corrections of order $(E/m_c)^2$ arise not only from the charm quarks in the sea, but also from the valence sector, since the charm quark propagates in the box diagrams. We note that the original derivation of the effective four-quark interaction is valid up to corrections of order $(E/m_c)^2$. The kaon-mixing amplitudes evaluated in the $N_f = 2 + 1$ and $2 + 1 + 1$ theories are thus subject to corrections of the same order in E/m_c as the derivation of the conventional four-quark interaction.

Regarding perturbative QCD corrections at the scale of the charm-quark mass on the amplitude in Eq. (94), the uncertainty on η_1 and η_3 factors is of $\mathcal{O}(\alpha_s(m_c)^3)$ [16, 17], while that on η_2 is of $\mathcal{O}(\alpha_s(m_c)^2)$ [85].⁶ On the other hand, the corrections of order $(E/m_c)^2$ due to dynamical charm-quark effects in the matching of the amplitudes are further suppressed by powers of $\alpha_s(m_c)$ and by a factor of $1/N_c$, given that they arise from quark-loop diagrams.

⁵We thank Martin Lüscher for an interesting discussion on this issue.

⁶The results of Ref. [15], based on the use of u - t unitarity for the two corresponding perturbative factors, also have an uncertainty of $\mathcal{O}(\alpha_s(m_c)^2)$ and $\mathcal{O}(\alpha_s(m_c)^3)$. The estimates for the missing higher-order contributions are, however, expected to be reduced with respect to the more traditional case where c - t unitarity is used; for a discussion on the $|\epsilon_K|$ computation in the u - t unitarity, see the relevant discussion in Sec. 6.1.

In order to make progress in resolving this so far uncontrolled systematic uncertainty, it is essential that any future calculation of B_K with $N_f = 2 + 1 + 1$ flavours properly addresses the size of these residual dynamical charm effects in a quantitative way.

Another issue in this context is how the lattice scale and the physical values of the quark masses are determined in the $2 + 1$ and $2 + 1 + 1$ flavour theories. Here it is important to consider in which way the quantities used to fix the bare parameters are affected by a dynamical charm quark.

A recent study [86] using three degenerate light quarks, together with a charm quark, indicates that the deviations between the $N_f = 3 + 1$ and the $N_f = 3$ theories are considerably below the 1% level in dimensionless quantities constructed from ratios of gradient-flow observables, such as t_0 and w_0 , used for scale setting. This study extends the nonperturbative investigations with two heavy mass-degenerate quarks [87, 88] which indicate that dynamical charm-quark effects in low-energy hadronic observables are considerably smaller than the expectation from a naive power counting in terms of $\alpha_s(m_c)$. For an additional discussion on this point, we refer to Ref. [83]. Given the hierarchy of scales between the charm-quark mass and that of B_K , we expect these errors to be modest. The ETM 15 $N_f = 2 + 1 + 1$ B_K result does not include an estimate of this systematic uncertainty. A more quantitative understanding will be required as the statistical uncertainties in B_K will be reduced. Within this review we will not discuss this issue further. However, we wish to point out that the present discussion also applies to $N_f = 2 + 1 + 1$ computations of the kaon BSM B -parameters discussed in Sec. 6.4.

A compilation of results for B_K with $N_f = 2 + 1 + 1$, $2 + 1$ and 2 flavours of dynamical quarks is shown in Tabs. 25 and 26, as well as Fig. 14. An overview of the quality of systematic error studies is represented by the colour coded entries in Tabs. 25 and 26. The values of the most relevant lattice parameters and comparative tables on the various estimates of systematic errors have been collected in the corresponding Appendices of the previous FLAG editions [89–91].

Since the last FLAG report, one new result for B_K appeared in RBC/UKQCD 24 [25].⁷ For the determination of B_K , the RBC/UKQCD Collaboration employs domain-wall fermions at three lattice spacings spanning the range $[0.07, 0.11]$ fm. For the two coarsest lattice spacings, simulations have been performed at the physical pion mass, whereas for the finest lattice spacing, a pion mass of about 230 MeV has been used. Residual chiral symmetry breaking effects induced by the finite extent of the 5th dimension in the domain-wall fermion formulation have been checked and found to contribute to the systematic uncertainty of the final estimate of B_K at the per-mille level. Finite-volume effects are found to be negligible. The renormalization constants of the lattice operators are determined nonperturbatively in two RI-SMOM schemes, namely (\not{d}, \not{d}) and (γ_μ, γ_μ) , corresponding to two different choices of renormalization conditions (see Ref. [23]). The final values of the renormalization constants are obtained from the average over the results of the two schemes. The error from the (γ_μ, γ_μ) scheme is used to quote the uncertainty arising from the lattice computation. The renormalization constants in the RI-SMOM schemes are computed at the renormalization scale $\mu = 2$ GeV. A nonperturbative step-scaling procedure is used to run them to $\mu = 3$ GeV where the results are perturbatively matched to the $\overline{\text{MS}}$ scheme. The continuum and physical

⁷We also mention the report of an ongoing work [92] related to the calculation of B_K in which the relevant operators are defined in the framework of gradient flow. A small flow time expansion method was applied in order to compute, to 1-loop approximation, the finite matching coefficients between the gradient flow and the $\overline{\text{MS}}$ schemes for the operators entering the B_K computation.

point result for B_K is obtained through a combined chiral and continuum extrapolation using NLO SU(2) chiral perturbation theory. The spread between the result obtained as described above and the result of a calculation performed directly at $\mu = 3$ GeV is taken as an estimate of the uncertainty due to discretization effects. The dominant error of the RBC/UKQCD 24 computation of B_K arises from the perturbative matching of the RI-SMOM schemes used in the lattice computation to the $\overline{\text{MS}}$ scheme. This is estimated as half the difference of the results obtained from the use of the two intermediate RI-SMOM schemes in the matching. In this computation of B_K , a green star symbol is assigned to all FLAG quality criteria.

For a detailed description of previous B_K calculations we refer the reader to FLAG 16 [90]. We now give the FLAG averages for B_K for $N_f = 2+1+1$, $2+1$, and 2 dynamical flavours.

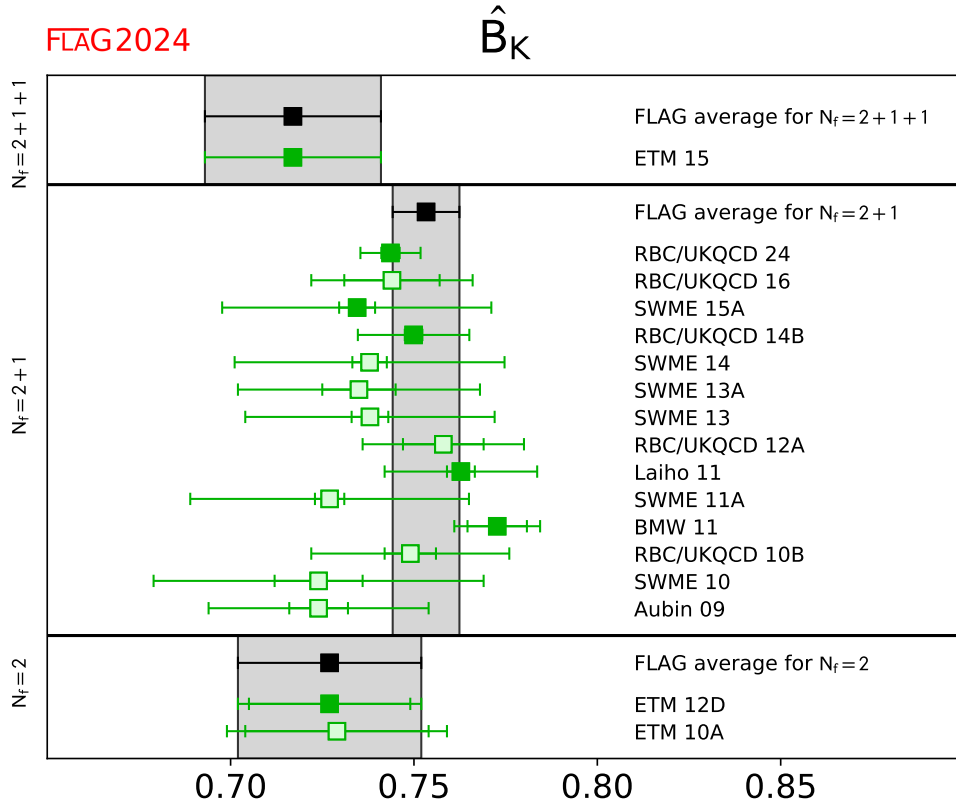


Figure 14: Unquenched lattice results for the RGI B -parameter \hat{B}_K . The grey bands indicate our averages described in the text. For $N_f = 2+1+1$ and $N_f = 2$ the FLAG averages coincide with the results by ETM 15 and ETM 12D, respectively.

We begin with the $N_f = 2+1$ global average, which is estimated by employing five different B_K results, namely BMW 11 [26], Laiho 11 [20], RBC/UKQCD 14B [23], SWME 15A [24], and RBC/UKQCD 24 [25]. Moreover, we recall that the expression of ϵ_K in terms of B_K is derived in the three-flavour theory (see Sec. 6.1). Our procedure is: first, we combine in quadrature the statistical and systematic errors of each individual result of the RGI B parameter \hat{B}_K . A weighted average is then obtained from the set of results. For the final error estimate, we take correlations between different collaborations into account. Specifically, we consider the statistical and finite-volume errors of SWME 15A and Laiho 11 to be correlated, since

both groups use the asqtad ensembles generated by the MILC Collaboration. Laiho 11 and RBC/UKQCD 14B both use domain-wall quarks in the valence sector and employ similar procedures for the nonperturbative determination of matching factors. Hence, we treat their quoted renormalization and matching uncertainties as correlated. Moreover, we treat the results obtained by RBC/UKQCD 14B and RBC/UKQCD 24 as fully correlated because part of the sea ensembles in the two calculations are common.⁸ In the calculation of the average, we incorporate the new FLAG data-driven criterion (see Sec. 2.1.2) concerning the extrapolation to the continuum limit which increases by approximately 3.7% the total error of the RBC/UKQCD 24 calculation. Following Schmelling's procedure [93] to construct the global covariance matrix of the results contributing to the average, we arrive at the following value, $\hat{B}_K = 0.7533(85)$. Since the fit implementing the weighted average has $\chi^2/\text{dof} = 1.142$, according to the general FLAG rule, we stretch the error by the square root of the reduced χ^2 value. This effect is mainly driven by the two most precise determinations of \hat{B}_K , corresponding to RBC/UKQCD 24 and BMW 11, which differ at the 2σ level. This procedure leads to the following result:

$$N_f = 2 + 1 : \quad \hat{B}_K = 0.7533(91) \quad \text{Refs. [20, 23–26]}, \quad (111)$$

After applying the NLO conversion factors $\hat{B}_K/B_K^{\overline{\text{MS}}}(2 \text{ GeV}) = 1.369$ and $\hat{B}_K/B_K^{\overline{\text{MS}}}(3 \text{ GeV}) = 1.415$ ⁹, this becomes

$$N_f = 2 + 1 : \quad B_K^{\overline{\text{MS}}}(2 \text{ GeV}) = 0.5503(66), \quad B_K^{\overline{\text{MS}}}(3 \text{ GeV}) = 0.5324(64), \quad \text{Refs. [20, 23–26]}. \quad (112)$$

Improvements in lattice calculations in recent years have led to a considerable reduction in statistical errors. This has implied that some of the results contributing to the global average are nowadays statistically incompatible. Only by taking into account the contributions to systemic uncertainties, both from the lattice calculations themselves and, notably, from perturbative matching, can it be seen that the weighted average produces a value of $\mathcal{O}(1)$ for the reduced χ^2 .

There is only a single result for $N_f = 2 + 1 + 1$, computed by the ETM collaboration [83]. Since it is free of red tags, it qualifies to the following average,

$$N_f = 2 + 1 + 1 : \quad \hat{B}_K = 0.717(18)(16), \quad \text{Ref. [83]}. \quad (113)$$

Using the same conversion factors as in the three-flavour theory, this value translates into

$$N_f = 2 + 1 + 1 : \quad B_K^{\overline{\text{MS}}}(2 \text{ GeV}) = 0.524(13)(12), \quad B_K^{\overline{\text{MS}}}(3 \text{ GeV}) = 0.507(13)(11), \quad \text{Ref. [83]}. \quad (114)$$

For $N_f = 2$ flavours the average is based on a single result, that of ETM 12D [94]:

$$N_f = 2 : \quad \hat{B}_K = 0.727(22)(12), \quad \text{Ref. [94]}, \quad (115)$$

which, using the same conversion factors as in the three-flavour theory, translates into

$$N_f = 2 : \quad B_K^{\overline{\text{MS}}}(2 \text{ GeV}) = 0.531(16)(9), \quad B_K^{\overline{\text{MS}}}(3 \text{ GeV}) = 0.514(16)(8), \quad \text{Ref. [94]}. \quad (116)$$

⁸However, due to partly different methodology in the analysis and the renormalization procedure the two computations are considered as separate, and for this reason they are both included in the global average.

⁹We refer to FLAG 19 [89] for a discussion of the procedure followed in estimating the conversion factors to $\overline{\text{MS}}$ at 2 GeV. In addition, for the computation of the conversion factor from RGI to the $\overline{\text{MS}}$ scheme at 3 GeV, which is new here, we have used the three-flavour Λ_{QCD} from FLAG 21 and the 4-loop formula for the β -function of the strong coupling constant. The propagation error owing to the error of Λ_{QCD} is found to be negligible compared to the total uncertainty of the B_K estimate.

Collaboration	Ref.	N_f	publication status	continuum extrapolation	chiral extrapolation	finite volume	renormalization	running	$B_K(\overline{\text{MS}}, 2 \text{ GeV})$	\hat{B}_K
ETM 15	[83]	2+1+1	A	★	○	○	★	a	0.524(13)(12)	0.717(18)(16) ¹
RBC/UKQCD 24	[25]	2+1	A	★	★	★	★	b	0.540(2)(20) ²	0.7436(25)(78)
RBC/UKQCD 16	[95]	2+1	A	○	○	○	★	c	0.543(9)(13) ³	0.744(13)(18) ⁴
SWME 15A	[24]	2+1	A	★	○	★	○ [‡]	–	0.537(4)(26)	0.735(5)(36) ⁵
RBC/UKQCD 14B	[23]	2+1	A	★	★	★	★	c	0.5478(18)(110) ³	0.7499(24)(150)
SWME 14	[22]	2+1	A	★	○	★	○ [‡]	–	0.5388(34)(266)	0.7379(47)(365)
SWME 13A	[96]	2+1	A	★	○	★	○ [‡]	–	0.537(7)(24)	0.735(10)(33)
SWME 13	[97]	2+1	C	★	○	★	○ [‡]	–	0.539(3)(25)	0.738(5)(34)
RBC/UKQCD 12A	[21]	2+1	A	○	★	○	★	c	0.554(8)(14) ³	0.758(11)(19)
Laiho 11	[20]	2+1	C	★	○	○	★	–	0.5572(28)(150)	0.7628(38)(205) ⁵
SWME 11A	[98]	2+1	A	★	○	○	○ [‡]	–	0.531(3)(27)	0.727(4)(38)
BMW 11	[26]	2+1	A	★	★	★	★	d	0.5644(59)(58)	0.7727(81)(84)
RBC/UKQCD 10B	[99]	2+1	A	○	○	★	★	e	0.549(5)(26)	0.749(7)(26)
SWME 10	[100]	2+1	A	★	○	○	○	–	0.529(9)(32)	0.724(12)(43)
Aubin 09	[101]	2+1	A	○	○	○	★	–	0.527(6)(21)	0.724(8)(29)

[‡] The renormalization is performed using perturbation theory at 1-loop, with a conservative estimate of the uncertainty.

a B_K is renormalized nonperturbatively at scales $1/a \sim 2.2\text{--}3.3$ GeV in the $N_f = 4$ RI/MOM scheme using two different lattice momentum scale intervals, the first around $1/a$ while the second around 3.5 GeV. The impact of the two ways to the final result is taken into account in the error budget. Conversion to $\overline{\text{MS}}$ is at 1-loop order at 3 GeV.

b B_K is renormalized nonperturbatively at a scale of 2.0 GeV in two RI/SMOM schemes for $N_f = 3$, and then run to 3 GeV using a nonperturbatively determined step-scaling function. A direct computation at 3 GeV is also used to estimate systematic uncertainties related to discretization effects. Conversion to $\overline{\text{MS}}$ is at 1-loop order at 3 GeV.

c B_K is renormalized nonperturbatively at a scale of 1.4 GeV in two RI/SMOM schemes for $N_f = 3$, and then run to 3 GeV using a nonperturbatively determined step-scaling function. Conversion to $\overline{\text{MS}}$ is at 1-loop order at 3 GeV.

d B_K is renormalized and run nonperturbatively to a scale of 3.5 GeV in the RI/MOM scheme. At the same scale, conversion at 1-loop order to $\overline{\text{MS}}$ is applied. Nonperturbative and NLO perturbative running agrees down to scales of 1.8 GeV within statistical uncertainties of about 2%.

e B_K is renormalized nonperturbatively at a scale of 2 GeV in two RI/SMOM schemes for $N_f = 3$, and then run to 3 GeV using a nonperturbatively determined step-scaling function. Conversion to $\overline{\text{MS}}$ is at 1-loop order at 3 GeV.

¹ $B_K(\overline{\text{MS}}, 2 \text{ GeV})$ and \hat{B}_K are related using the conversion factor 1.369, i.e., the one obtained with $N_f = 2 + 1$.

² $B_K(\overline{\text{MS}}, 2 \text{ GeV})$ value from a private communication with the authors. The first error is due to lattice statistical and systematic uncertainties; the second error is associated with the perturbative truncation uncertainty in matching to $\overline{\text{MS}}$ at a scale of 2 GeV.

³ $B_K(\overline{\text{MS}}, 2 \text{ GeV})$ is obtained from the estimate for \hat{B}_K using the conversion factor 1.369.

⁴ \hat{B}_K is obtained from $B_K(\overline{\text{MS}}, 3 \text{ GeV})$ using the conversion factor employed in Ref. [23].

⁵ \hat{B}_K is obtained from the estimate for $B_K(\overline{\text{MS}}, 2 \text{ GeV})$ using the conversion factor 1.369.

Table 25: Results for the kaon B -parameter in QCD with $N_f = 2 + 1 + 1$ and $N_f = 2 + 1$, together with a summary of systematic errors. Information about nonperturbative running is indicated in the column “running,” with details given at the bottom of the table.

Collaboration	Ref.	N_f	publication status	continuum extrapolation	chiral extrapolation	finite volume	renormalization	running	$B_K(\overline{\text{MS}}, 2 \text{ GeV})$	\hat{B}_K
ETM 12D	[94]	2	A	★	○	○	★	f	0.531(16)(9)	0.727(22)(12) ¹
ETM 10A	[102]	2	A	★	○	○	★	g	0.533(18)(12) ¹	0.729(25)(17)

f B_K is renormalized nonperturbatively at scales $1/a \sim 2\text{--}3.7$ GeV in the $N_f = 2$ RI/MOM scheme. In this scheme, nonperturbative and NLO perturbative running are shown to agree from 4 GeV down to 2 GeV to better than 3% [102, 103].

g B_K is renormalized nonperturbatively at scales $1/a \sim 2\text{--}3$ GeV in the $N_f = 2$ RI/MOM scheme. In this scheme, nonperturbative and NLO perturbative running are shown to agree from 4 GeV down to 2 GeV to better than 3% [102, 103].

¹ $B_K(\overline{\text{MS}}, 2 \text{ GeV})$ and \hat{B}_K are related using the conversion factor 1.369, i.e., the one obtained with $N_f = 2 + 1$.

Table 26: Results for the kaon B -parameter in QCD with $N_f = 2$, together with a summary of systematic errors. Information about nonperturbative running is indicated in the column “running,” with details given at the bottom of the table.

6.4 Kaon BSM B -parameters

We now consider the matrix elements of operators that encode the effects of physics beyond the Standard Model (BSM) to the mixing of neutral kaons. In this theoretical framework, both the SM and BSM contributions add up to reproduce the experimentally observed value of ϵ_K . As long as BSM contributions involve heavy particles with masses much larger than Λ_{QCD} , they will be short-distance dominated. The effective Hamiltonian for generic $\Delta S = 2$ processes including BSM contributions reads

$$\mathcal{H}_{\text{eff,BSM}}^{\Delta S=2} = \sum_{i=1}^5 C_i(\mu) Q_i(\mu), \quad (117)$$

where Q_1 is the four-quark operator of Eq. (91) that gives rise to the SM contribution to ϵ_K . In the so-called SUSY basis introduced by Gabbiani et al. [104], the operators Q_2, \dots, Q_5 are¹⁰

$$\begin{aligned} Q_2 &= (\bar{s}^a(1 - \gamma_5)d^a)(\bar{s}^b(1 - \gamma_5)d^b), \\ Q_3 &= (\bar{s}^a(1 - \gamma_5)d^b)(\bar{s}^b(1 - \gamma_5)d^a), \\ Q_4 &= (\bar{s}^a(1 - \gamma_5)d^a)(\bar{s}^b(1 + \gamma_5)d^b), \\ Q_5 &= (\bar{s}^a(1 - \gamma_5)d^b)(\bar{s}^b(1 + \gamma_5)d^a), \end{aligned} \quad (118)$$

¹⁰Thanks to QCD parity invariance lattice computations for three more dimension-six operators, whose parity conserving parts coincide with the corresponding parity conserving contributions of the operators Q_1, Q_2 and Q_3 , can be ignored.

where a and b are colour indices. In analogy to the case of B_K , one then defines the B -parameters of Q_2, \dots, Q_5 according to

$$B_i(\mu) = \frac{\langle \bar{K}^0 | Q_i(\mu) | K^0 \rangle}{N_i \langle \bar{K}^0 | \bar{s} \gamma_5 d | 0 \rangle \langle 0 | \bar{s} \gamma_5 d | K^0 \rangle}, \quad i = 2, \dots, 5. \quad (119)$$

The factors $\{N_2, \dots, N_5\}$ are given by $\{-5/3, 1/3, 2, 2/3\}$, and it is understood that $B_i(\mu)$ is specified in some renormalization scheme, such as $\overline{\text{MS}}$ or a variant of the regularization-independent momentum subtraction (RI-MOM) scheme.

The SUSY basis has been adopted in Refs. [25, 83, 94, 95, 105]. Alternatively, one can employ the chiral basis of Buras, Misiak and Urban [106]. The SWME collaboration prefers the latter since the anomalous dimension that enters the RG running has been calculated to 2-loop order in perturbation theory [106]. Results obtained in the chiral basis can be easily converted to the SUSY basis via

$$B_3^{\text{SUSY}} = \frac{1}{2} \left(5B_2^{\text{chiral}} - 3B_3^{\text{chiral}} \right). \quad (120)$$

The remaining B -parameters are the same in both bases. In the following, we adopt the SUSY basis and drop the superscript.

Older quenched results for the BSM B -parameters can be found in Refs. [107–109]. For a nonlattice approach to get estimates for the BSM B -parameters see Ref. [110].

Estimates for B_2, \dots, B_5 have been reported for QCD with $N_f = 2$ (ETM 12D [94]), $N_f = 2 + 1$ (RBC/UKQCD 12E [105], SWME 13A [96], SWME 14C [111], SWME 15A [24], RBC/UKQCD 16 [95, 112], RBC/UKQCD 24 [25]) and $N_f = 2 + 1 + 1$ (ETM 15 [83]) flavours of dynamical quarks. Since the publication of FLAG 19 [89] a single new work Ref. [25] has appeared. The basic characteristics of this calculation have been reported in the B_K section, see Sec. 6.3. As in the case of B_K , the dominant error for all the BSM B -parameters arises from the systematic uncertainty associated to the truncation error in the perturbative matching from the intermediate schemes to the $\overline{\text{MS}}$ scheme. This is estimated as half the difference of the results obtained from the matching to $\overline{\text{MS}}$ of the two intermediate schemes. The ratio of the BSM to SM matrix elements are also reported in Ref. [25].

All the available results are listed and compared in Tab. 27 and Fig. 15. In general, one finds that the BSM B -parameters computed by different collaborations do not show the same level of consistency as the SM kaon-mixing parameter B_K discussed previously. Control over the systematic uncertainties from chiral and continuum extrapolations as well as finite-volume effects in B_2, \dots, B_5 is expected to be at a comparable level as that for B_K , as far as the results by ETM 12D, ETM 15, SWME 15A and RBC/UKQCD 16 are concerned, since the set of gauge ensembles employed in both kinds of computations is the same. However, the most recent results by RBC/UKQCD 24 with $N_f = 2 + 1$ flavours are, in general, much more precise than the older ones. Notice that the calculation by RBC/UKQCD 12E has been performed at a single value of the lattice spacing and a minimum pion mass of 290 MeV.

As reported in RBC/UKQCD 16 [95] and RBC/UKQCD 24 [25], the comparison of results obtained in the conventional RI-MOM and in two RI-SMOM schemes shows significant discrepancies for some of the BSM B -parameters. Tensions are observed for the cases of B_4 and B_5 , where the discrepancies between results obtained with RI-MOM and RI-SMOM are at the level of 2.6σ and 4.5σ , respectively. The results of RBC/UKQCD 16 and RBC/UKQCD 24 lie closer to those of SWME 15A which rely on perturbative renormalization at 1-loop order. On the other hand, the results for B_2 and B_3 obtained by ETM 15, SWME 15A, RBC/UKQCD 16 and RBC/UKQCD 24 show a better level of compatibility.

The findings by RBC/UKQCD 16 [95], RBC/UKQCD 17A [112] and RBC/UKQCD 24 [25] highlight the importance of carefully assessing the systematic effects on the implementation of the Rome-Southampton method used for nonperturbative renormalization. In particular, the RI-MOM and RI-SMOM schemes differ in that the use of nonexceptional kinematics, in the RI-SMOM scheme, removes the need to subtract the pseudo-Goldstone boson pole contamination, as is required in the RI-MOM case. In addition, for each of the schemes a specific analysis of the truncation error in the perturbative matching to $\overline{\text{MS}}$ must be carried out.

Collaboration	Ref. N_f	publication status	continuum extrapolation	chiral extrapolation	finite volume	renormalization	running	B_2	B_3	B_4	B_5
ETM 15	[83] 2+1+1	A	★	○	○	★	a	0.46(1)(3)	0.79(2)(5)	0.78(2)(4)	0.49(3)(3)
RBC/UKQCD 24	[25] 2+1	A	★	★	★	★	b	0.4794(25)(35)	0.746(13)(17)	0.897(02)(10)	0.6882(78)(94)
RBC/UKQCD 16	[95] 2+1	A	○	○	○	★	b	0.488(7)(17)	0.743(14)(65)	0.920(12)(16)	0.707(8)(44)
SWME 15A	[24] 2+1	A	★	○	★	○ [†]	–	0.525(1)(23)	0.773(6)(35)	0.981(3)(62)	0.751(7)(68)
SWME 14C	[111] 2+1	C	★	○	★	○ [†]	–	0.525(1)(23)	0.774(6)(64)	0.981(3)(61)	0.748(9)(79)
SWME 13A [†]	[96] 2+1	A	★	○	★	○ [†]	–	0.549(3)(28)	0.790(30)	1.033(6)(46)	0.855(6)(43)
RBC/UKQCD 12E	[105] 2+1	A	■	○	★	★	b	0.43(1)(5)	0.75(2)(9)	0.69(1)(7)	0.47(1)(6)
ETM 12D	[94] 2	A	★	○	○	★	c	0.47(2)(1)	0.78(4)(2)	0.76(2)(2)	0.58(2)(2)

[†] The renormalization is performed using perturbation theory at 1-loop order, with a conservative estimate of the uncertainty.

a B_i are renormalized nonperturbatively at scales $1/a \sim 2.2\text{--}3.3$ GeV in the $N_f = 4$ RI/MOM scheme using two different lattice momentum scale intervals, with values around $1/a$ for the first and around 3.5 GeV for the second one. The impact of these two ways to the final result is taken into account in the error budget. Conversion to $\overline{\text{MS}}$ is at 1-loop order at 3 GeV.

b The B -parameters are renormalized nonperturbatively at a scale of 3 GeV.

c B_i are renormalized nonperturbatively at scales $1/a \sim 2\text{--}3.7$ GeV in the $N_f = 2$ RI/MOM scheme using two different lattice momentum scale intervals, with values around $1/a$ for the first and around 3 GeV for the second one.

[‡] The computation of B_4 and B_5 has been revised in Refs. [24] and [111].

Table 27: Results for the BSM B -parameters B_2, \dots, B_5 in the $\overline{\text{MS}}$ scheme at a reference scale of 3 GeV. Information about nonperturbative running is indicated in the column “running,” with details given at the bottom of the table.

A nonperturbative computation of the running of the four-fermion operators contributing to the B_2, \dots, B_5 parameters has been carried out with two dynamical flavours using the Schrödinger functional renormalization scheme [28]. Renormalization matrices of the operator basis are used to build step-scaling functions governing the continuum-limit running between hadronic and electroweak scales. A comparison to perturbative results using NLO (2-loop order) for the four-fermion operator anomalous dimensions indicates that, at scales of about 3 GeV, nonperturbative effects can induce a sizeable contribution to the running. Similar conclusions are obtained on the basis of preliminary results for the renormalization-group running of the complete basis of $\Delta F = 2$ four-fermion operators using $N_f = 3$ dynamical massless flavours in the Schrödinger setup [29].

A closer look at the calculations reported in ETM 15 [83], SWME 15A [24], RBC/UKQCD 16 [95], and RBC/UKQCD 24 [25] reveals that cutoff effects tend to be larger for the BSM B -parameters compared to those of B_K . In order to take into account this effect in the average analysis, we make use of the new FLAG data-driven criterion (see Sec. 2.1.2) concerning the extrapolation to the continuum limit. In summary, we report that in the average procedure, (a) for B_2 the total errors by RBC/UKQCD 24 and RBC/UKQCD 16 have been inflated by a factor 2.6 and by 22%, respectively; (b) for B_3 the total errors by ETM 15, RBC/UKQCD 16 and RBC/UKQCD 24 have been inflated by 11%, 45% and 52%, respectively; (c) for B_4 no error inflation is required; and (d) for B_5 the total errors by SWME 15A and RBC/UKQCD 16 have been inflated by 3% and 24%, respectively.

Finally we present our estimates for the BSM B -parameters, quoted in the $\overline{\text{MS}}$ -scheme at scale 3 GeV. For $N_f = 2+1$ our estimate is given by the average of the results from SWME 15A, RBC/UKQCD 16, and RBC/UKQCD 24. In our analysis, the results in RBC/UKQCD 16 and RBC/UKQCD 24, though obtained through partially different analyses, are considered as fully correlated because some gauge ensembles are common in the two computations. We find $B_2 = 0.488(12)$ ($\chi^2/\text{dof} = 1.58$); $B_3 = 0.757(27)$ ($\chi^2/\text{dof} = 0.17$); $B_4 = 0.903(12)$ ($\chi^2/\text{dof} = 1.36$); $B_5 = 0.691(14)$ ($\chi^2/\text{dof} = 0.43$). Following the FLAG rule, for cases that have a value of the reduced χ^2 greater than unity, we use the square root of the latter to stretch the respective error. Hence our averages are

$$\begin{aligned} N_f = 2 + 1 : \\ B_2 = 0.488(15), \quad B_3 = 0.757(27), \quad B_4 = 0.903(14), \quad B_5 = 0.691(14), \quad \text{Refs. [24, 25, 95].} \end{aligned} \tag{121}$$

For $N_f = 2+1+1$ and $N_f = 2$, our estimates coincide—with one exception—with the ones by ETM 15 and ETM 12D, respectively, since there is only one computation for each case. Only for the case of B_3 with $N_f = 2+1+1$, owing to the application of the $\delta(a_{\min})$ criterion the error of the average estimate is inflated by about 11% with respect to the ETM 15 reported value. Thus we quote

$$\begin{aligned} N_f = 2 + 1 + 1 : \\ B_2 = 0.46(1)(3), \quad B_3 = 0.79(6), \quad B_4 = 0.78(2)(4), \quad B_5 = 0.49(3)(3), \quad \text{Ref. [83],} \end{aligned} \tag{122}$$

$$\begin{aligned} N_f = 2 : \\ B_2 = 0.47(2)(1), \quad B_3 = 0.78(4)(2), \quad B_4 = 0.76(2)(2), \quad B_5 = 0.58(2)(2), \quad \text{Ref. [94].} \end{aligned} \tag{123}$$

Based on the above discussion about the effects of employing different intermediate momentum subtraction schemes in the nonperturbative renormalization of the operators, there is

evidence that the discrepancy in the B_4 and B_5 results between $N_f = 2, 2 + 1 + 1$, and $N_f = 2 + 1$ calculations should not be directly attributed to an effect of the number of dynamical flavours. To clarify the present situation, it would be important to perform a direct comparison of results by the ETM collaboration obtained both with RI-MOM and RI-SMOM methods. A calculation based on a different nonperturbative renormalization scheme, such as the Schrödinger functional, would provide valuable information to shed light on the current situation.

In closing, we encourage authors to provide the correlation matrix of the B_i parameters—as done in Ref. [25]—since this information is required in phenomenological studies of New Physics scenarios.

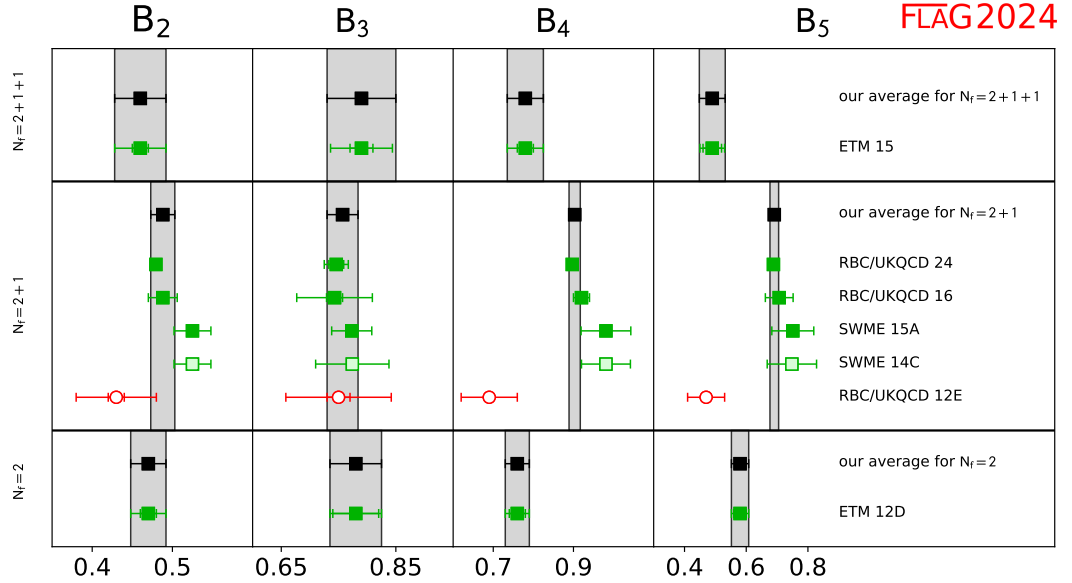


Figure 15: Results for the BSM B -parameters defined in the $\overline{\text{MS}}$ scheme at a reference scale of 3 GeV (see Tab. 27).

References

- [1] G.C. Branco, L. Lavoura and J.P. Silva, *CP violation*, *Int. Ser. Monogr. Phys.* **103** (1999) 1.

- [2] M. Sozzi, *Discrete Symmetries and CP Violation: From Experiment to Theory*, *Oxford University Press* (2008) 1.
- [3] A. Buras, *Gauge Theories of Weak Decays*, *Cambridge University Press* (2020) 1.
- [4] G. Buchalla, A.J. Buras and M.E. Lautenbacher, *Weak decays beyond leading logarithms*, *Rev. Mod. Phys.* **68** (1996) 1125 [[hep-ph/9512380](#)].
- [5] A.J. Buras, *Weak Hamiltonian, CP violation and rare decays*, [hep-ph/9806471](#), Published in *Les Houches 1997, Probing the standard model of particle interactions*, Pt. 1, 281-539.
- [6] L. Lellouch, *Flavor physics and lattice quantum chromodynamics*, in *Modern perspectives in lattice QCD: Quantum field theory and high performance computing. Proceedings, International School, 93rd Session, Les Houches, France, August 3-28, 2009*, pp. 629–698, 2011 [[1104.5484](#)].
- [7] [FLAG 21] Y. Aoki et al., *FLAG Review 2021*, *Eur. Phys. J. C* **82** (2022) 869 [[2111.09849](#)].
- [8] K. Anikeev et al., *B physics at the Tevatron: Run II and beyond*, [hep-ph/0201071](#).
- [9] U. Nierste, *Three lectures on meson mixing and CKM phenomenology, published in Dubna 2008, Heavy Quark Physics (HQP08)*, pp. 1-39, [0904.1869](#).
- [10] A.J. Buras and D. Guadagnoli, *Correlations among new CP violating effects in $\Delta F = 2$ observables*, *Phys. Rev.* **D78** (2008) 033005 [[0805.3887](#)].
- [11] A.J. Buras, D. Guadagnoli and G. Isidori, *On ϵ_K beyond lowest order in the operator product expansion*, *Phys. Lett.* **B688** (2010) 309 [[1002.3612](#)].
- [12] PARTICLE DATA GROUP collaboration, *Review of particle physics*, *Phys. Rev. D* **110** (2024) 030001.
- [13] T. Inami and C.S. Lim, *Effects of superheavy quarks and leptons in low-energy weak processes $K_L \rightarrow \mu\bar{\mu}$, $K^+ \rightarrow \pi^+\nu\bar{\nu}$ and $K^0 \leftrightarrow \bar{K}^0$* , *Prog. Theor. Phys.* **65** (1981) 297.
- [14] [RBC/UKQCD 12F] N. H. Christ, T. Izubuchi, C.T. Sachrajda, A. Soni and J. Yu, *Long distance contribution to the KL-KS mass difference*, *Phys. Rev.* **D88** (2013) 014508 [[1212.5931](#)].
- [15] J. Brod, M. Gorbahn and E. Stamou, *Standard-model prediction of ϵ_K with manifest CKM unitarity*, *Phys. Rev. Lett.* **125** (2020) 171803 [[1911.06822](#)].
- [16] J. Brod and M. Gorbahn, *Next-to-next-to-leading-order charm-quark contribution to the CP violation parameter ϵ_K and ΔM_K* , *Phys.Rev.Lett.* **108** (2012) 121801 [[1108.2036](#)].
- [17] J. Brod and M. Gorbahn, *ϵ_K at next-to-next-to-leading order: the charm-top-quark contribution*, *Phys. Rev.* **D82** (2010) 094026 [[1007.0684](#)].
- [18] G. Martinelli, C. Pittori, C.T. Sachrajda, M. Testa and A. Vladikas, *A general method for nonperturbative renormalization of lattice operators*, *Nucl. Phys.* **B445** (1995) 81 [[hep-lat/9411010](#)].

- [19] M. Lüscher, R. Narayanan, P. Weisz and U. Wolff, *The Schrödinger functional: a renormalizable probe for non-abelian gauge theories*, *Nucl. Phys.* **B384** (1992) 168 [[hep-lat/9207009](#)].
- [20] J. Laiho and R.S. Van de Water, *Pseudoscalar decay constants, light-quark masses and B_K from mixed-action lattice QCD*, *PoS LATTICE2011* (2011) 293 [[1112.4861](#)].
- [21] [RBC/UKQCD 12] R. Arthur et al., *Domain wall QCD with near-physical pions*, *Phys.Rev.* **D87** (2013) 094514 [[1208.4412](#)].
- [22] [SWME 14] T. Bae et al., *Improved determination of B_K with staggered quarks*, *Phys. Rev.* **D89** (2014) 074504 [[1402.0048](#)].
- [23] [RBC/UKQCD 14B] T. Blum et al., *Domain wall QCD with physical quark masses*, *Phys. Rev.* **D93** (2016) 074505 [[1411.7017](#)].
- [24] [SWME 15A] Y.-C. Jang et al., *Kaon BSM B -parameters using improved staggered fermions from $N_f = 2 + 1$ unquenched QCD*, *Phys. Rev.* **D93** (2016) 014511 [[1509.00592](#)].
- [25] [RBC/UKQCD 24] P. Boyle, Felix, J.M. Flynn, N. Garron, J. Kettle, R. Mukherjee et al., *Kaon mixing beyond the standard model with physical masses*, *Phys. Rev. D* **110** (2024) 034501 [[2404.02297](#)].
- [26] [BMW 11] S. Dürr, Z. Fodor, C. Hoelbling, S. Katz, S. Krieg et al., *Precision computation of the kaon bag parameter*, *Phys.Lett.* **B705** (2011) 477 [[1106.3230](#)].
- [27] [ALPHA 07A] P. Dimopoulos et al., *Non-perturbative renormalisation of $\Delta F = 2$ four-fermion operators in two-flavour QCD*, *JHEP* **0805** (2008) 065 [[0712.2429](#)].
- [28] [ALPHA 18B] P. Dimopoulos et al., *Non-Perturbative Renormalisation and Running of BSM Four-Quark Operators in $N_f = 2$ QCD*, *Eur. Phys. J.* **C78** (2018) 579 [[1801.09455](#)].
- [29] I. Campos Plasencia, M. Dalla Brida, G.M. de Divitiis, A. Lytle, R. Marinelli, M. Papinutto et al., *Non-perturbative mixing and renormalisation of $\Delta F=2$ Four-Fermion Operators*, *PoS LATTICE2023* (2024) 270.
- [30] L. Wolfenstein, *Parametrization of the Kobayashi-Maskawa Matrix*, *Phys. Rev. Lett.* **51** (1983) 1945.
- [31] Z. Bai, N.H. Christ, J.M. Karpie, C.T. Sachrajda, A. Soni and B. Wang, *Long-distance contribution to ϵ_K from lattice QCD*, *Phys. Rev. D* **109** (2024) 054501 [[2309.01193](#)].
- [32] [SWME 23A] S. Jwa et al., *2023 update of ϵ_K with lattice QCD inputs*, *PoS LATTICE2023* (2024) 160 [[2312.02986](#)].
- [33] J. Brod, S. Kvedaraitė, Z. Polonsky and A. Youssef, *Electroweak corrections to the Charm-Top-Quark Contribution to ϵ_K* , *JHEP* **12** (2022) 014 [[2207.07669](#)].
- [34] [SWME 14D] W. Lee et al., *Current status of ϵ_K calculated with lattice QCD inputs*, *PoS LATTICE2014* (2014) 371 [[1410.6995](#)].

- [35] [SWME 15B] J. A. Bailey, Y.-C. Jang, W. Lee and S. Park, *Standard Model evaluation of ε_K using lattice QCD inputs for \hat{B}_K and V_{cb}* , *Phys. Rev.* **D92** (2015) 034510 [[1503.05388](#)].
- [36] [SWME 18] J.A. Bailey et al., *Updated evaluation of ϵ_K in the standard model with lattice QCD inputs*, *Phys. Rev.* **D98** (2018) 094505 [[1808.09657](#)].
- [37] UTFIT collaboration, *New UFit Analysis of the Unitarity Triangle in the Cabibbo-Kobayashi-Maskawa scheme*, *Rend. Lincei Sci. Fis. Nat.* **34** (2023) 37 [[2212.03894](#)].
- [38] A.J. Buras and J. Girrbach, *Stringent tests of constrained Minimal Flavor Violation through $\Delta F = 2$ transitions*, *Eur. Phys. J. C* **73** (2013) 2560 [[1304.6835](#)].
- [39] [SWME 25A] S. Jwa et al., *2024 update of ε_K with lattice QCD inputs*, *PoS LATTICE2024* (2024) 433 [[2501.00215](#)].
- [40] [SWME 25B] S. Jwa et al., *2025 update on ε_K in the Standard Model with lattice QCD inputs*, [2503.00351](#).
- [41] S. Hashimoto, *Inclusive semi-leptonic B meson decay structure functions from lattice QCD*, *PTEP* **2017** (2017) 053B03 [[1703.01881](#)].
- [42] M.T. Hansen, H.B. Meyer and D. Robaina, *From deep inelastic scattering to heavy-flavor semileptonic decays: Total rates into multihadron final states from lattice QCD*, *Phys. Rev. D* **96** (2017) 094513 [[1704.08993](#)].
- [43] P. Gambino and S. Hashimoto, *Inclusive Semileptonic Decays from Lattice QCD*, *Phys. Rev. Lett.* **125** (2020) 032001 [[2005.13730](#)].
- [44] P. Gambino, S. Hashimoto, S. Mächler, M. Panero, F. Sanfilippo, S. Simula et al., *Lattice QCD study of inclusive semileptonic decays of heavy mesons*, *JHEP* **07** (2022) 083 [[2203.11762](#)].
- [45] A. Barone, S. Hashimoto, A. Jüttner, T. Kaneko and R. Kellermann, *Approaches to inclusive semileptonic $B_{(s)}$ -meson decays from Lattice QCD*, *JHEP* **07** (2023) 145 [[2305.14092](#)].
- [46] O. Cata and S. Peris, *Long distance dimension eight operators in $B(K)$* , *JHEP* **03** (2003) 060 [[hep-ph/0303162](#)].
- [47] M. Ciuchini, E. Franco, V. Lubicz, G. Martinelli, L. Silvestrini and C. Tarantino, *Power corrections to the CP-violation parameter ε_K* , *JHEP* **02** (2022) 181 [[2111.05153](#)].
- [48] V. Cirigliano, A. Pich, G. Ecker and H. Neufeld, *Isospin violation in epsilon-prime*, *Phys. Rev. Lett.* **91** (2003) 162001 [[hep-ph/0307030](#)].
- [49] V. Cirigliano, H. Gisbert, A. Pich and A. Rodríguez-Sánchez, *Isospin-violating contributions to ϵ'/ϵ* , *JHEP* **02** (2020) 032 [[1911.01359](#)].
- [50] [RBC/UKQCD 20] R. Abbott et al., *Direct CP violation and the $\Delta I = 1/2$ rule in $K \rightarrow \pi\pi$ decay from the Standard Model*, *Phys. Rev. D* **102** (2020) 054509 [[2004.09440](#)].

- [51] PARTICLE DATA GROUP collaboration, *Review of Particle Physics*, [*PTEP* **2020** \(2020\) 083C01](#).
- [52] [RBC/UKQCD 15G] Z. Bai et al., *Standard Model Prediction for Direct CP Violation in $K \rightarrow \pi\pi$ Decay*, [*Phys. Rev. Lett.* **115** \(2015\) 212001 \[1505.07863\]](#).
- [53] [RBC/UKQCD 15F] T. Blum et al., *$K \rightarrow \pi\pi$ $\Delta I = 3/2$ decay amplitude in the continuum limit*, [*Phys. Rev.* **D91** \(2015\) 074502 \[1502.00263\]](#).
- [54] PARTICLE DATA GROUP collaboration, *Review of Particle Physics*, [*Phys. Rev.* **D98** \(2018\) 030001](#).
- [55] Z. Bai, *Long distance part of ϵ_K from lattice QCD*, [*PoS LATTICE2016* \(2017\) 309 \[1611.06601\]](#).
- [56] Z. Bai, N.H. Christ, T. Izubuchi, C.T. Sachrajda, A. Soni and J. Yu, *$K_L - K_S$ Mass Difference from Lattice QCD*, [*Phys. Rev. Lett.* **113** \(2014\) 112003 \[1406.0916\]](#).
- [57] N.H. Christ, X. Feng, G. Martinelli and C.T. Sachrajda, *Effects of finite volume on the $K_L - K_S$ mass difference*, [*Phys. Rev.* **D91** \(2015\) 114510 \[1504.01170\]](#).
- [58] B. Wang, *Calculation of the $K_L - K_S$ mass difference for physical quark masses*, [*PoS LATTICE2019* \(2019\) 093 \[2001.06374\]](#).
- [59] B. Wang, *Calculating Δm_K with lattice QCD*, [*PoS LATTICE2021* \(2022\) 141 \[2301.01387\]](#).
- [60] [RBC/UKQCD 23A] T. Blum, P.A. Boyle, D. Horying, T. Izubuchi, L. Jin, C. Jung et al., *$\Delta I = 3/2$ and $\Delta I = 1/2$ channels of $K \rightarrow \pi\pi$ decay at the physical point with periodic boundary conditions*, [*Phys. Rev. D* **108** \(2023\) 094517 \[2306.06781\]](#).
- [61] Z. Bai et al., *Erratum: Standard-Model Prediction for Direct CP Violation in $K \rightarrow \pi\pi$ Decay*, [1603.03065](#).
- [62] [RBC/UKQCD 23B] T. Blum et al., *Isospin 0 and 2 two-pion scattering at physical pion mass using all-to-all propagators with periodic boundary conditions in lattice QCD*, [*Phys. Rev. D* **107** \(2023\) 094512 \[2301.09286\]](#).
- [63] M. Gaillard and B.W. Lee, *$\Delta I = 1/2$ Rule for Nonleptonic Decays in Asymptotically Free Field Theories*, [*Phys. Rev. Lett.* **33** \(1974\) 108](#).
- [64] G. Altarelli and L. Maiani, *Octet Enhancement of Nonleptonic Weak Interactions in Asymptotically Free Gauge Theories*, [*Phys. Lett. B* **52** \(1974\) 351](#).
- [65] [RBC/UKQCD 21] T. Blum et al., *Lattice determination of $I = 0$ and 2 $\pi\pi$ scattering phase shifts with a physical pion mass*, [*Phys. Rev. D* **104** \(2021\) 114506 \[2103.15131\]](#).
- [66] N. Ishizuka, K.I. Ishikawa, A. Ukawa and T. Yoshié, *Calculation of $K \rightarrow \pi\pi$ decay amplitudes with improved Wilson fermion action in lattice QCD*, [*Phys. Rev.* **D92** \(2015\) 074503 \[1505.05289\]](#).

- [67] N. Ishizuka, K.I. Ishikawa, A. Ukawa and T. Yoshié, *Calculation of $K \rightarrow \pi\pi$ decay amplitudes with improved Wilson fermion action in non-zero momentum frame in lattice QCD*, *Phys. Rev. D* **D98** (2018) 114512 [[1809.03893](#)].
- [68] A. Donini, P. Hernández, C. Pena and F. Romero-López, *Nonleptonic kaon decays at large N_c* , *Phys. Rev. D* **D94** (2016) 114511 [[1607.03262](#)].
- [69] A. Donini, P. Hernández, C. Pena and F. Romero-López, *Dissecting the $\Delta I = 1/2$ rule at large N_c* , *Eur. Phys. J. C* **80** (2020) 638 [[2003.10293](#)].
- [70] J. Baeza-Ballesteros, P. Hernández and F. Romero-López, *A lattice study of $\pi\pi$ scattering at large N_c* , *JHEP* **06** (2022) 049 [[2202.02291](#)].
- [71] N. Christ and X. Feng, *Including electromagnetism in $K \rightarrow \pi\pi$ decay calculations*, *EPJ Web Conf.* **175** (2018) 13016 [[1711.09339](#)].
- [72] Y. Cai and Z. Davoudi, *QED-corrected Lellouch-Luescher formula for $K \rightarrow \pi\pi$ decay*, *PoS LATTICE2018* (2018) 280 [[1812.11015](#)].
- [73] N. Christ, X. Feng, J. Karpie and T. Nguyen, *π - π scattering, QED, and finite-volume quantization*, *Phys. Rev. D* **106** (2022) 014508 [[2111.04668](#)].
- [74] D. Bećirević et al., *$K^0 \bar{K}^0$ mixing with Wilson fermions without subtractions*, *Phys. Lett. B* **B487** (2000) 74 [[hep-lat/0005013](#)].
- [75] [ALPHA 01] R. Frezzotti, P.A. Grassi, S. Sint and P. Weisz, *Lattice QCD with a chirally twisted mass term*, *JHEP* **08** (2001) 058 [[hep-lat/0101001](#)].
- [76] [ALPHA 06] P. Dimopoulos et al., *A precise determination of B_K in quenched QCD*, *Nucl. Phys. B* **B749** (2006) 69 [[hep-ph/0601002](#)].
- [77] [ALPHA 07] P. Dimopoulos et al., *Flavour symmetry restoration and kaon weak matrix elements in quenched twisted mass QCD*, *Nucl. Phys. B* **B776** (2007) 258 [[hep-lat/0702017](#)].
- [78] R.S. Van de Water and S.R. Sharpe, *B_K in staggered chiral perturbation theory*, *Phys. Rev. D* **D73** (2006) 014003 [[hep-lat/0507012](#)].
- [79] J.A. Bailey, H.-J. Kim, W. Lee and S.R. Sharpe, *Kaon mixing matrix elements from beyond-the-Standard-Model operators in staggered chiral perturbation theory*, *Phys. Rev. D* **D85** (2012) 074507 [[1202.1570](#)].
- [80] P.H. Ginsparg and K.G. Wilson, *A remnant of chiral symmetry on the lattice*, *Phys. Rev. D* **D25** (1982) 2649.
- [81] Y. Aoki et al., *The Kaon B -parameter from quenched domain-wall QCD*, *Phys. Rev. D* **73** (2006) 094507 [[hep-lat/0508011](#)].
- [82] [RBC/UKQCD] N. Christ, *Estimating domain wall fermion chiral symmetry breaking*, *PoS LAT2005* (2006) 345.

- [83] [ETM 15] N. Carrasco, P. Dimopoulos, R. Frezzotti, V. Lubicz, G.C. Rossi, S. Simula et al., $\Delta S = 2$ and $\Delta C = 2$ bag parameters in the standard model and beyond from $N_f = 2 + 1 + 1$ twisted-mass lattice QCD, *Phys. Rev.* **D92** (2015) 034516 [[1505.06639](#)].
- [84] V. Cirigliano, J.F. Donoghue and E. Golowich, *Dimension eight operators in the weak OPE*, *JHEP* **10** (2000) 048 [[hep-ph/0007196](#)].
- [85] A.J. Buras, M. Jamin and P.H. Weisz, *Leading and next-to-leading QCD corrections to ϵ parameter and $B_0 - \bar{B}_0$ mixing in the presence of a heavy top quark*, *Nucl. Phys.* **B347** (1990) 491.
- [86] [ALPHA 20] R. Höllwieser, F. Knechtli and T. Korzec, *Scale setting for $N_f = 3 + 1$ QCD*, *Eur. Phys. J. C* **80** (2020) 349 [[2002.02866](#)].
- [87] [ALPHA 14A] M. Bruno, J. Finkenrath, F. Knechtli, B. Leder and R. Sommer, *Effects of Heavy Sea Quarks at Low Energies*, *Phys. Rev. Lett.* **114** (2015) 102001 [[1410.8374](#)].
- [88] A. Athenodorou, J. Finkenrath, F. Knechtli, T. Korzec, B. Leder, M.K. Marinkovic et al., *How perturbative are heavy sea quarks?*, *Nucl. Phys.* **B943** (2019) 114612 [[1809.03383](#)].
- [89] [FLAG 19] S. Aoki et al., *FLAG Review 2019: Flavour Lattice Averaging Group (FLAG)*, *Eur. Phys. J. C* **80** (2020) 113 [[1902.08191](#)].
- [90] [FLAG 16] S. Aoki et al., *Review of lattice results concerning low-energy particle physics*, *Eur. Phys. J. C* **77** (2017) 112 [[1607.00299](#)].
- [91] [FLAG 13] S. Aoki, Y. Aoki, C. Bernard, T. Blum, G. Colangelo et al., *Review of lattice results concerning low-energy particle physics*, *Eur.Phys.J.* **C74** (2014) 2890 [[1310.8555](#)].
- [92] A. Suzuki, Y. Taniguchi, H. Suzuki and K. Kanaya, *Four quark operators for kaon bag parameter with gradient flow*, *Phys. Rev. D* **102** (2020) 034508 [[2006.06999](#)].
- [93] M. Schmelling, *Averaging correlated data*, *Phys.Scripta* **51** (1995) 676.
- [94] [ETM 12D] V. Bertone et al., *Kaon Mixing Beyond the SM from $N_f=2$ tmQCD and model independent constraints from the UTA*, *JHEP* **03** (2013) 089 [[1207.1287](#)], [Erratum: JHEP07,143(2013)].
- [95] [RBC/UKQCD 16] N. Garron, R.J. Hudspith and A.T. Lytle, *Neutral Kaon Mixing Beyond the Standard Model with $n_f = 2 + 1$ Chiral Fermions Part 1: Bare Matrix Elements and Physical Results*, *JHEP* **11** (2016) 001 [[1609.03334](#)].
- [96] [SWME 13A] T. Bae et al., *Neutral kaon mixing from new physics: matrix elements in $N_f = 2 + 1$ lattice QCD*, *Phys. Rev.* **D88** (2013) 071503 [[1309.2040](#)].
- [97] [SWME 13] T. Bae et al., *Update on B_K and ϵ_K with staggered quarks*, *PoS LATTICE2013* (2013) 476 [[1310.7319](#)].
- [98] [SWME 11A] T. Bae et al., *Kaon B -parameter from improved staggered fermions in $N_f = 2 + 1$ QCD*, *Phys.Rev.Lett.* **109** (2012) 041601 [[1111.5698](#)].

- [99] [RBC/UKQCD 10B] Y. Aoki et al., *Continuum limit of B_K from 2+1 flavor domain wall QCD*, *Phys.Rev.* **D84** (2011) 014503 [[1012.4178](#)].
- [100] [SWME 10] T. Bae et al., *B_K using HYP-smeared staggered fermions in $N_f = 2 + 1$ unquenched QCD*, *Phys. Rev.* **D82** (2010) 114509 [[1008.5179](#)].
- [101] C. Aubin, J. Laiho and R.S. Van de Water, *The neutral kaon mixing parameter B_K from unquenched mixed-action lattice QCD*, *Phys. Rev.* **D81** (2010) 014507 [[0905.3947](#)].
- [102] [ETM 10A] M. Constantinou et al., *BK -parameter from $N_f = 2$ twisted mass lattice QCD*, *Phys. Rev.* **D83** (2011) 014505 [[1009.5606](#)].
- [103] [ETM 10C] M. Constantinou et al., *Non-perturbative renormalization of quark bilinear operators with $N_f = 2$ (tmQCD) Wilson fermions and the tree- level improved gauge action*, *JHEP* **08** (2010) 068 [[1004.1115](#)].
- [104] F. Gabbiani, E. Gabrielli, A. Masiero and L. Silvestrini, *A Complete analysis of FCNC and CP constraints in general SUSY extensions of the standard model*, *Nucl. Phys.* **B477** (1996) 321 [[hep-ph/9604387](#)].
- [105] [RBC/UKQCD 12E] P. A. Boyle, N. Garron and R.J. Hudspith, *Neutral kaon mixing beyond the standard model with $n_f = 2 + 1$ chiral fermions*, *Phys. Rev.* **D86** (2012) 054028 [[1206.5737](#)].
- [106] A.J. Buras, M. Misiak and J. Urban, *Two loop QCD anomalous dimensions of flavor changing four quark operators within and beyond the standard model*, *Nucl. Phys.* **B586** (2000) 397 [[hep-ph/0005183](#)].
- [107] C.R. Allton, L. Conti, A. Donini, V. Gimenez, L. Giusti, G. Martinelli et al., *B parameters for Delta $S = 2$ supersymmetric operators*, *Phys. Lett.* **B453** (1999) 30 [[hep-lat/9806016](#)].
- [108] A. Donini, V. Gimenez, L. Giusti and G. Martinelli, *Renormalization group invariant matrix elements of Delta $S = 2$ and Delta $I = 3/2$ four fermion operators without quark masses*, *Phys. Lett.* **B470** (1999) 233 [[hep-lat/9910017](#)].
- [109] R. Babich, N. Garron, C. Hoelbling, J. Howard, L. Lellouch and C. Rebbi, *$K0 - \text{anti-}K0$ mixing beyond the standard model and CP-violating electroweak penguins in quenched QCD with exact chiral symmetry*, *Phys. Rev.* **D74** (2006) 073009 [[hep-lat/0605016](#)].
- [110] A.J. Buras and J.-M. Gérard, *Dual QCD Insight into BSM Hadronic Matrix Elements for $K^0 - \bar{K}^0$ Mixing from Lattice QCD*, *Acta Phys. Polon.* **B50** (2019) 121 [[1804.02401](#)].
- [111] [SWME 14C] J. Leem et al., *Calculation of BSM Kaon B -parameters using Staggered Quarks*, *PoS LATTICE2014* (2014) 370 [[1411.1501](#)].
- [112] [RBC/UKQCD 17A] P. Boyle et al., *Neutral kaon mixing beyond the Standard Model with $n_f = 2 + 1$ chiral fermions. Part 2: non perturbative renormalisation of the $\Delta F = 2$ four-quark operators*, *JHEP* **10** (2017) 054 [[1708.03552](#)].